Commun Nonlinear Sci Numer Simulat 131 (2024) 107846

Contents lists available at ScienceDirect

Communications in Nonlinear Science and Numerical Simulation

journal homepage: www.elsevier.com/locate/cnsns

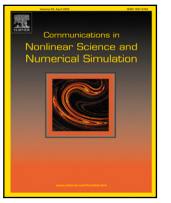

Research paper

# Multistable states in a predator–prey model with generalized Holling type III functional response and a strong Allee effect

Yanni Zeng, Pei Yu *

*Department of Mathematics, Western University, London, Ontario, N6A 5B7, Canada*

ARTICLE INFO

*MSC:*
34C05
34C23
34C60
34D23

*Keywords:*
Predator-prey model
Parametric analysis
Hopf bifurcation
Limit cycle
Multistable states

ABSTRACT

In this paper, we present a complete parametric analysis on a nonlinear predator–prey system with the generalized Holling type III functional response and a strong Allee effect. We apply the hierarchical parametric analysis to derive explicit conditions for the existence and stability of equilibrium solutions in a 5-dimensional parameter space. Specifically, a detailed study on Hopf bifurcation is given to show bifurcation of multiple limit cycles, and complex dynamics of multistable states including bistable, tristable and tetrastable phenomena. We also conduct simulations and provide a biological interpretation of the multistable states under various conditions.

## 1. Introduction

Different species living together in an area constitute an ecological community whose populations are greatly affected by their interspecific relationship with other organisms. Among various kinds of interspecific relationships, the predation relationship forms the basis of the food chain and energy circle in the ecosystem, and it can be very complicated. Consequently, predator–prey dynamics is an essential mathematical biology topic, and extensive researches have been conducted. One of the classic frameworks used to describe predator–prey dynamics of two species is the so-called Gause-type predator–prey model [1,2] governed by the following two nonlinear ordinary differential equations:

$$\begin{aligned} \dot{x} &= g(x)x - p(x,y)y, \\ \dot{y} &= c\,p(x,y)y - q(y)y, \end{aligned} \tag{1}$$

with the initial conditions, $x(0) \geq 0$ and $y(0) \geq 0$, where the dot represents differentiation with respect to time $t$, $x = x(t)$ and $y = y(t)$ denote the prey and predator population densities at time $t$, respectively. The positive functions $g(x)$ and $q(y)$ describe the growth rate of prey and the mortality rate of the predator in the absence of the other species. The function $p(x,y)$ is known as functional responses describing the consumption rate of a given prey by its predator as a function of their density [3,4]. In general, the functional responses can mainly be classified into three types (Holling I, II, III) [5,6]. The Holling Type I functional response,

$$p(x) = \alpha x,$$

was first used in the Lotka–Volterra model [7,8], which is a linear function that will increase boundlessly. However, the boundless linear relationship is not realistic in the natural world.

* Corresponding author.
*E-mail addresses:* yzeng243@uwo.ca (Y. Zeng), pyu@uwo.ca (P. Yu).

https://doi.org/10.1016/j.cnsns.2024.107846
Received 28 August 2023; Received in revised form 5 January 2024; Accepted 8 January 2024
Available online 11 January 2024

The Holling Type II functional response [5]

$$p(x) = \frac{\alpha x}{\alpha T_h x + 1},$$

further considers the handling time $T_h$ associated with the prey, where $\alpha$ is the attack rate. This is a hyperbolic increasing function and will reach a saturated state.

The generalized Holling Type III [9] is defined as

$$p(x) = \frac{mx^2}{ax^2 + bx + 1},$$

in which the parameters $a$ and $m$ take positive values, but $b$ can be negative satisfying $b > -2\sqrt{a}$ to ensure that $ax^2 + bx + 1 > 0$ for $x > 0$, and $\lim_{x\to\infty} p(x) = \frac{m}{a}$. Note that the cases $b \geq 0$ and $b < 0$ are slightly different. For both cases, the "learning behavior" occurs in the predators, describing the case that the predators learn to concentrate on the prey as its population increases, which was proved by the experimental work conducted by Hassell [10] for several predation cases in invertebrate predators. They modeled the Holling type III functional response by considering the attack rate in the Holling Type II functional response as

$$\alpha(x) = \frac{mx}{1 + bx}.$$

Another interesting phenomenon in predation for the generalized Holling Type III model occurs when $b < 0$: the consumption rate continues to increase until it reaches the maximum and then starts decreasing, approaching $\frac{m}{a}$. This is attributed to the phenomenon known as "group defense" [11] in prey, which refers to the collaborative behavior that provides protection from predators. Their defensive capabilities improve as the population size increases.

The growth rate of a single species is often assumed in the form of logistic type $g(x) = r(1 - \frac{x}{K})$, implying that the species grows faster when the density is low and decreases when the density is high due to limitations of resources. However, such an assumption may not be realistic since the growth of the species is also affected by other factors such as difficulties in mating, unable to defend as a group and social felicitation of reproduction, etc. [12]. In 1931, the concept "Allee effect" [13–15] was proposed to explain why a decrease appears in the population growth rate at low population density. The concept was further classified as strong and weak Allee effects. The weak Allee effect describes the situation that the growth rate is decreasing when density is low, but it is still positive; while the strong Allee effect implies that the growth rate decreases when the density is low and reaches negative values. In other words, for the strong Allee effect, the species might be extinct if the population density is lower than a critical threshold.

A commonly used function for one species population growth rate is to modify the logistic growth rate by including the Allee effect, known as the multiplicative Allee effect [12,16],

$$g(x) = r\left(1 - \frac{x}{K}\right)(x - e),$$

where $e$ represents the Allee effect threshold and $K$ is the carrying capacity, and the restriction $|e| < K$ is usually assumed. The strong and weak Allee effects are then specified by $0 < e < K$ and $-K < e < 0$, respectively [17–19]. Many researchers have studied predator–prey systems with the Allee effect and different functional responses, such as Holling type II [20]. Gonzrález–Olivares [21] showed the existence of multiple limit cycles in a predator–prey model with Holling type III functional response and the Allee Effect added, while a further study is needed to consider the number of bifurcating limit cycles due to a strong Allee effect. Up to now, the predator–prey systems with generalized Holling type III and the Allee effect have not been investigated in detail.

This paper considers predator–prey systems with the generalized Holling type III functional responses and the strong Allee effect. It is assumed that the Allee effect threshold is far from the carrying capacity [22], i.e., the restriction $e \in (0, \frac{K}{2})$ is imposed on the model under consideration. The model is written as

$$\begin{aligned} \dot{x} &= rx\left(1 - \frac{x}{K}\right)(x - e) - \frac{mx^2 y}{ax^2 + bx + 1}, \\ \dot{y} &= y\left(\frac{mcx^2}{ax^2 + bx + 1} - d\right), \end{aligned} \tag{2}$$

where $m$ is the capturing rate of the predator, $c$ is the positive constant specifying conservation efficiency rate of prey to predator. The conditions $e \in (0, \frac{K}{2})$ and $b > -2\sqrt{a}$ are required for the aforementioned biological meaning. This model describes the case that the risk of extinction is significant, and the predator's consumption rate grows slowly when the population density is low. Then, the consumption rate will increase as the prey population increases, finally reaching a saturated state.

To simplify the analysis, introducing the following scaling,

$$x = KX, \quad y = \frac{rY}{m}, \quad \tau = rKt,$$

into (2) we obtain the dimensionless system,

$$\begin{aligned} \dot{X} &= X(1 - X)(X - E) - \frac{X^2 Y}{AX^2 + BX + 1}, \\ \dot{Y} &= Y\left(\frac{CX^2}{AX^2 + BX + 1} - D\right), \end{aligned} \tag{3}$$

where the new parameters are defined as $A = K^2 a$, $C = \frac{mKc}{r}$, $D = \frac{d}{rK}$ and $E = \frac{e}{K}$, all of them take positive values, and $B > -2\sqrt{A}$, $0 < E < \frac{1}{2}$, which defines a critical Allee effect value relative to the carrying capacity. In this paper, we will use the hierarchical

parametric analysis developed in [23] to study the stability and bifurcation of system (3), in particular, on Hopf bifurcation to derive explicit conditions under which Hopf bifurcation can occur, associated with multistable states, including bistable, tristable and tetrastable phenomena.

The rest of this paper is organized as follows. The bounded region of the system solutions and the existence of equilibrium points are discussed in Section 2. In Section 3, the analysis of the stability and bifurcation of equilibria are presented, especially Hopf bifurcation is analyzed. Simulations are given in Section 4 for possible multistable scenarios. Finally, the conclusion and discussion are provided in Section 5.

## 2. Equilibrium solutions of system (3)

### 2.1. System without the Allee effect

The dynamics of the predator–prey model system (3) with the generalized Holling type III functional response, but without the Allee effect, has been well studied in [24]. For the convenience of a comparison, we list the main results on the stability and bifurcation of this model, taken from [24] as follows.

(i) $\mathrm{E}_0 : (X_0, Y_0) = (0,0) :$ Saddle,

(ii) $\mathrm{E}_1 : (X_1, Y_1) = (1,0) :$ Stable node (saddle) for $C < C_{\mathrm{t}}$ $(C > C_{\mathrm{t}})$, $C_{\mathrm{t}} = D(A + B + 1)$,

(iii) ——

(iv) $\mathrm{E}_3 : (X_3, Y_3) = \left(X_3, \frac{C}{D} X_3(1 - X_3)\right)$,

where $0 < X_3 < 1$ with $X_3$ being the positive roots of the quadratic polynomial $F_1(X_3)$, given by

$$F_1(X_3) = (C - AD)X_3^2 - BDX_3 - D. \tag{4}$$

The analysis and conditions on the existence and stability of $\mathrm{E}_3$ are complex, see more details in [24]. Note that we purposely skip $\mathrm{E}_2$ in the equilibria to conveniently compare with that of the system with the Allee effect.

With the strong Allee effect added, the dynamics of the system (3), especially the stability of the equilibria, will change. For example, we will show that the extinction equilibrium $(0,0)$ completely changes its stability when the strong Allee effect is present. That is, it is always a stable node.

### 2.2. System with the Allee effect

To study the equilibria of system (3), we first define

$$\Omega = \left\{(X,Y) \mid X > 0,\ Y > 0,\ Y < C \max\left\{\tfrac{1-E}{D}, 1\right\} - CX\right\},$$

which is the positive invariant and trapping region for the flows of system (3) in the first quadrant of the $X$-$Y$ plane. The proof to find the bounded region is included in the previous research [25]. Based on that, the system (3) has the following four equilibrium solutions:

(i) the extinction equilibrium $\mathrm{E}_0 :$ $(X_0, Y_0) = (0,0)$,

(ii) the predator free equilibrium $\mathrm{E}_1 :$ $(X_1, Y_1) = (1,0)$,

(iii) the predator free equilibrium $\mathrm{E}_2 :$ $(X_2, Y_2) = (E,0)$,

(iv) the coexistence equilibrium $\mathrm{E}_3 :$ $(X_3, Y_3)$, where

$$Y_3 = \frac{C}{D} X_3(1 - X_3)(X_3 - E),\ \left(E < X_3 < 1\right),$$

and $X_3$ is determined from the same quadratic equation $F_1(X_3) = 0$, indicating that this quadratic equation does not change with the Allee effect added, but the equilibrium $\mathrm{E}_3$ is different due to the change of $Y_3$. Solving $F_1 = 0$ gives two solutions:

$$X_{3\pm} = \frac{1}{2(C - AD)}(BD \pm \sqrt{\Delta}), \quad \text{where} \quad \Delta = B^2D^2 + 4D(C - AD). \tag{5}$$

The condition $E < X_3 < 1$ is required to guarantee that $Y_3 > 0$.

It is easy to get from $\Delta \geq 0$ that $\mathrm{E}_3$ exists only if $C \geq C_{\mathrm{SN}} = D(A - \frac{B^2}{4})$. When $B \geq 0$, $F_1 = 0$ has positive solutions only if $C > AD$, leading to that $X_{3+} > 0$ and $X_{3-} < 0$. The equilibrium $\mathrm{E}_3$ can be represented by a graph of parabola plotted on the $C$-$X_3$ plane, with a unique vertex defined at

$$(C_{\mathrm{SN}}, X_{\mathrm{SN}}) = \left(D\left(A - \frac{B^2}{4}\right), -\frac{2}{B}\right),$$

where SN denotes Saddle Node. Further, it is straightforward to show that $X_3$ is monotonically increasing for $X_3 > X_{\mathrm{SN}}$ and monotonically decreasing as C increases for $X_3 < X_{\mathrm{SN}}$ by examining the derivative,

$$\frac{\mathrm{d}C_{\mathrm{H}}}{\mathrm{d}X_3} = -D\left(\frac{B}{X_3^2} + \frac{2}{X_3^3}\right),$$

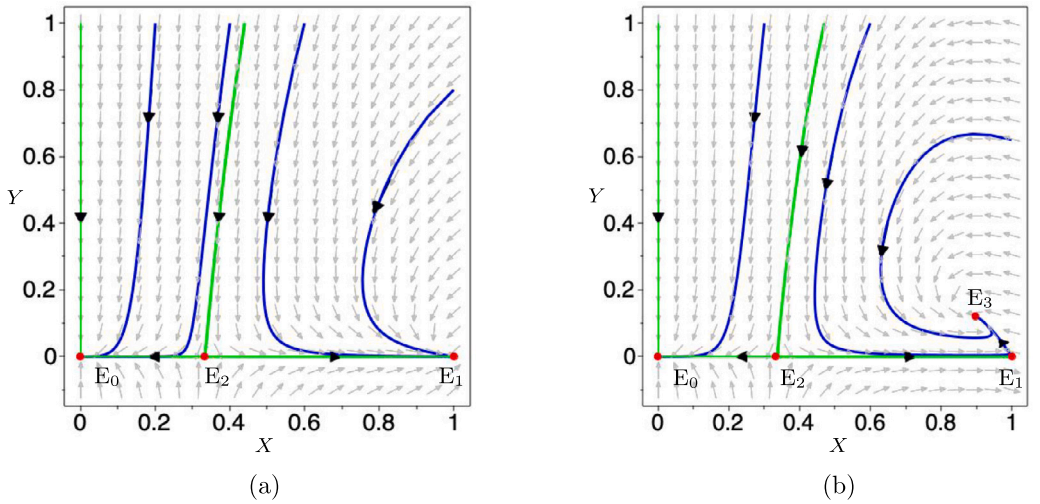


**Fig. 1.** Simulated phase portraits of system (3) for $(A, B, D, E) = (\frac{1}{2}, \frac{1}{2}, 1, \frac{1}{3})$, showing the stable node $E_0$ and the saddle $E_2$, and $E_1$ being (a) a stable node when $C = 1$; and (b) a saddle when $C = 2.3$.

where $C_H$ is solved from $F_1 = 0$ for $C$, where the subscript H represents Hopf. The existence conditions of $E_{3\pm}$ can be described as

$$X_3 \in (E, 1) = \begin{cases} X_3^+ = \dfrac{BD + \sqrt{\Delta}}{2(C - AD)}, & \text{for } B \geq 0,\ C > AD \\ & \text{or } \max\{-2\sqrt{A}, -\frac{2}{E}\} < B < 0,\ C \geq C_{SN}; \\ X_3^- = \dfrac{BD - \sqrt{\Delta}}{2(C - AD)}, & \text{for } -2\sqrt{A} < B < -2,\ C_{SN} \leq C < AD. \end{cases} \tag{6}$$

The special case $C = AD$ is included in the case $C \geq C_{SN}, B < 0$, since

$$\lim_{h=C-AD\to 0} \frac{BD + \sqrt{\Delta}}{2(C - AD)} \overset{H}{=} \lim_{h\to 0} \frac{4D}{4\sqrt{B^2D^2 + 4Dh}} = -\frac{1}{B},$$

which requires $\max\{-2\sqrt{A}, -\frac{1}{E}\} < B < -1$. Hence, it is seen from (6) that only $X_{3-}$ exists for $X_{SN} < E < X_{3-} < 1$ and only $X_{3+}$ exists for $E < X_{3+} < 1 < X_{SN}$; while both $E_{3+}$ and $E_{3-}$ exist if $E < X_{SN} < 1$. In other words, only $E_{3-}$ exists if $-2\sqrt{A} < B < -\frac{2}{E}$; only $E_{3+}$ exists if $B > \max\{-2, -2\sqrt{A}\}$; and both $E_{3+}$ and $E_{3-}$ exist if $\max\{-2\sqrt{A}, -\frac{2}{E}\} < B < -2$, satisfying $E < X_{3+} < X_{SN} < X_{3-} < 1$.

## 3. Stability and bifurcation analysis

### 3.1. Boundary equilibria

First, note that the three boundary equilibria, $E_0$, $E_1$ and $E_2$ always exist for all admissible parameters values. To obtain the stability of these equilibria, we compute the Jacobian Matrix of system (3) at these three equilibria to obtain

$$J(E_0) = \begin{pmatrix} -E & 0 \\ 0 & -D \end{pmatrix}, \quad J(E_1) = \begin{pmatrix} -(1-E) & -\frac{1}{A+B+1} \\ 0 & \frac{C}{A+B+1} - D \end{pmatrix}, \quad J(E_2) = \begin{pmatrix} E(1-E) & -\frac{E^2}{AE^2+BE+1} \\ 0 & \frac{CE^2}{AE^2+BE+1} - D \end{pmatrix}. \tag{7}$$

It is clear to see from $J(E_0)$ that $E_0$ is a stable note, i.e., it is asymptotically stable (AS). $J(E_1)$ has a negative eigenvalue, $\lambda_{11} = E - 1$, and its second eigenvalue equals $\lambda_{12} = \frac{C}{A+B+1} - D$, implying that $\lambda_{12} \gtrless 0$ if $0 < C \gtrless C_t = D(A + B + 1)$. For $J(E_2)$, one of its eigenvalues is positive, $\lambda_{21} = E(1 - E)$. In summary, we have the following result.

**Lemma 1.** *The predator–prey model (3) has three boundary equilibria* $E_0$, $E_1$ *and* $E_2$. $E_0$ *is always* AS *(a stable node) and* $E_2$ *is always unstable (either a saddle or an unstable node); while* $E_1$

(i) *is a saddle if* $C > C_t$;
(ii) *is a stable focus if* $C < C_t$; *and*
(iii) *has a transcritical bifurcation with* $E_3$ *at the critical point* $C = C_t$.

An example of simulated phase portraits for system (3) showing the three equilibria is depicted in Fig. 1.

### 3.2. Positive equilibrium

In this subsection, we consider the stability of the positive equilibrium $\mathrm{E}_3$ and possible Hopf and Bogdanov–Takens bifurcations from this equilibrium. For convenience, in the following study, we define the positive equilibrium as

$$\mathrm{E}_3 = (\mathrm{X}_{3\pm}, \mathrm{Y}_{3\pm}). \tag{8}$$

We also define three critical values of $B$: $B_1$, $B_2$ and $B_s$, where $B_1$ is determined from the equation $R_1 = 0$, given by

$$\begin{aligned} R_1 =& (E^2+E+1)^4B^4 - 4(E+1)(E^6-3E^5-38E^4+21E^3-38E^2-3E+1)B^3 \\ &+ 6(E^6-20E^5+168E^4-150E^3+168E^2-20E+1)B^2 \\ &- 4(E+1)(E^4-51E^3+40E^2-51E+1)B + E^4-92E^3+70E^2-92E+1, \\ B_2 =& -\frac{2}{E}\left(1+E-\sqrt{1-E+E^2}\right), \\ B_s =& -\frac{1}{E}\left(1+2E-\sqrt{1-E+E^2}\right), \end{aligned} \tag{9}$$

as well as the critical values on other parameters $E, C$, as well as on $X_3$:

$$\begin{aligned} E_t^* =& \ 0.35056501\cdots, \\ C_E =& \ D\left(A+\tfrac{B}{E}+\tfrac{1}{E^2}\right), \\ \overline{X}_3 =& \ \frac{1}{3}\left(\sqrt{E^2-E+1}+1+E\right), \\ A_{\mathrm{H}}(X_3) =& \ \frac{2BX_3^3+(1-B-BE)X_3^2-E}{-[3X_3^2-2(1+E)X_3+E]X_3^2}. \end{aligned} \tag{10}$$

In the following, we shall use the values $A_{\mathrm{H}}(X_3 = X_M) = A_{\mathrm{H}}^M$ and $A_{\mathrm{H}}(X_3 = X_m) = A_{\mathrm{H}}^m$, where $X_M$ and $X_m$ ($X_M < X_m$) are the solutions of $G_3(X_3) = 0$, with $G_3$ given by

$$G_3(X_3) = 3BX_3^5 - 3(BE+B-1)X_3^4 + \left[(E^2+E+1)B - E - 1\right]X_3^3 - 6EX_3^2 + 3E(E+1)X_3 - E^2. \tag{11}$$

Note that $A_{\mathrm{H}}$ gains its maximal and minimal values at $X_M$ and $X_m$, respectively.

When $C = C_t$, $F_1 = 0$ has two solutions: $X_3 = 1$ and $X_3 = X_t = -\frac{1}{B+1}$.

It is easy to show that $\mathrm{E}_{3-}$ is a saddle if it exists. The stability of $\mathrm{E}_{3+}$ is much more complex. For convenience, for bifurcation analysis on $\mathrm{E}_{3+}$, we treat $C$ as the bifurcation parameter and other parameters $A, B, D$ and $E$ as control parameters. Further, it can be shown that at most three Hopf bifurcation points are possible by varying the parameter $C$ with fixed values of the control parameters. For simplicity, we denote the Hopf critical points as $\mathrm{E}_{3\mathrm{H}_1} = (\mathrm{X}_{\mathrm{H}_1}, \mathrm{Y}_{\mathrm{H}_1})$, $\mathrm{E}_{3\mathrm{H}_2} = (\mathrm{X}_{\mathrm{H}_2}, \mathrm{Y}_{\mathrm{H}_2})$ and $\mathrm{E}_{3\mathrm{H}_3} = (\mathrm{X}_{\mathrm{H}_3}, \mathrm{Y}_{\mathrm{H}_3})$ when the bifurcation parameter $C$ equals $C_{\mathrm{H}_1}$, $C_{\mathrm{H}_2}$ and $C_{\mathrm{H}_3}$, respectively.

We have the following theorem.

**Theorem 2.** *System (3) has a saddle–node bifurcation at the critical point $C = C_{\mathrm{SN}}$ from $\mathrm{E}_3$. The equilibrium $\mathrm{E}_{3-}$ is a saddle when it exists. System (3) undergoes Hopf bifurcation from $\mathrm{E}_{3+}$ under the conditions described below.*

(A) *When $B > \max\{B_2, -2\sqrt{A}\}$, $E_{3+}$ is* AS *for $\overline{X}_3 < X_{3+} < \min\{1, X_{\mathrm{SN}}\}$. Further, if*

(A-1) *$B \geq B_1$, then one Hopf bifurcation occurs at $C_{\mathrm{H}_1}$, for which $E_{3+}$ is* AS *for $C \in (C_{\mathrm{SN}}, C_{\mathrm{H}_1})$, and unstable for $(C_{\mathrm{H}_1}, C_E)$;*

(A-2) *$B < B_1$, then*

(a) *either one Hopf bifurcation exists at $C_{\mathrm{H}_1}$ if $A \in (0, A_{\mathrm{H}}^m] \cup [A_{\mathrm{H}}^M, +\infty)$, and $\mathrm{E}_{3+}$ has the same stability condition as that given in* (A-1)*;*

(b) *or three Hopf bifurcations exist at $C_{\mathrm{H}_1}, C_{\mathrm{H}_2}$ and $C_{\mathrm{H}_3}$ if $A \in (A_{\mathrm{H}}^m, A_{\mathrm{H}}^M)$, for which $\mathrm{E}_{3+}$ is* AS *for $C \in (C_{\mathrm{SN}}, C_{\mathrm{H}_1}) \cup (C_{\mathrm{H}_2}, C_{\mathrm{H}_3})$, and unstable for $C \in (C_{\mathrm{H}_1}, C_{\mathrm{H}_2}) \cup (C_{\mathrm{H}_3}, C_E)$.*

(B) *When $\max\{-\frac{2}{E}, -2\sqrt{A}\} < B \leq B_2$, if*

(B-1) *$A > A_{\mathrm{H}}^M$, then $\mathrm{E}_{3+}$ is unstable;*

(B-2) *$\frac{B^2}{4} < A < A_{\mathrm{H}}^M$, then two Hopf bifurcations exist, where $\mathrm{E}_{3+}$ is* AS *for $C \in (C_{\mathrm{H}_1}, C_{\mathrm{H}_2})$ and unstable for $C \in (C_{\mathrm{SN}}, C_{\mathrm{H}_1}) \cup (C_{\mathrm{H}_2}, C_E)$.*

*Bogdanov–Takens bifurcation occurs from the equilibrium,*

$$(X_3, Y_3) = \left(-\frac{2}{B}, \frac{2C(B+2)(EB+2)}{DB^3}\right),$$

*at the critical point, defined by*

$$A = \frac{B^2D+4C}{4D}, \quad E = -\frac{4(B+3)}{B(B+4)}, \quad 0 < E < \frac{1}{2}.$$

**Proof.** Based on the existence condition of $E_3$ obtained in the previous section, we first let $C = C_H(X_3)$ represent the solution of $F_1(X_3) = 0$. Then, calculating the Jacobian of system (3) at $E_3$, where $E_3$ represents both $E_{3+}$ and $E_{3-}$, yields the trace and determinant, given by

$$\mathrm{tr}(J(E_3)) = \frac{\mathrm{tr}_1 + AX_3^2\mathrm{tr}_2}{AX_3^2 + BX_3 + 1}, \tag{12}$$

and

$$\det(J(E_3)) = \frac{D(1 - X_3)(X_3 - E)(BX_3 + 2)}{AX_3^2 + BX_3 + 1}, \tag{13}$$

respectively, where

$$\begin{aligned} \mathrm{tr}_1 &= BX_3^2(1 + E - 2X_3) - (X_3^2 - E), \\ \mathrm{tr}_2 &= -3X_3^2 + 2(1 + E)X_3 - E. \end{aligned} \tag{14}$$

It follows from $B > -2\sqrt{A}$ that $AX_3^2 + BX_3 + 1 > (\sqrt{A}X_3 - 1)^2 \geq 0$. Further, from the existence condition (6) for $E_{3-}$, we obtain $BX_{3-} + 2 < 0$, leading to $\det(J_{3-}) < 0$. Thus, $E_{3-}$ is a saddle when it exists. Similarly, we have $\det(J_{3+}) > 0$ since $C > C_{SN}$, showing that the stability of $E_{3+}$ depends on $\mathrm{tr}(J_{3+})$ and a saddle–node bifurcation occurs when $X_3 = X_{SN} = -\frac{2}{B}$ and $C = C_{SN} = D\left(A - \frac{B^2}{4}\right)$. The necessary conditions for existence of B-T bifurcation from $E_3$ can be easily obtained by solving $\det(J(E_3)) = \mathrm{tr}(J(E_3)) = 0$, yielding the same conditions given in Theorem 2.

In the following, we will use $\mathrm{tr}(J_{3+})$ to study the stability and bifurcation of $E_{3+}$ according to two cases: (A) $B > \max\{B_2, -2\sqrt{A}\}$, and (B) $\max\{-2\sqrt{A}, -\frac{2}{E}\} < B < B_2$. Because $B = B_2$ is the critical point at which $\overline{X}_3 = X_{SN}$, where $\overline{X}_3$ is the unique biologically meaningful solution of $\mathrm{tr}_2 = 0$. For $-2\sqrt{A} < B < B_2$, the solution $\overline{X}_3$ does not belong to the equilibrium $E_{3+}$. For convenience, we will use the notations $X_3 = X_{3+}$ and $E_3 = E_{3+}$ in the following analysis. We consider two cases.

**Case 1:** $B > \max\{B_2, -2\sqrt{A}\}$. We first show that under the condition (A-1), $E_3$ is AS for $\overline{X}_3 < X_3 < \min\{1, X_{SN}\}$. Note that by comparing $-\frac{2}{X_3}$ with $-2\sqrt{A}$, the condition can be further divided into two subcases: $X_3\sqrt{A} > 1$ and $X_3\sqrt{A} < 1$.

For the case $X_3\sqrt{A} > 1$, we only need to consider $B > -\frac{2}{X_3}$ since $-2\sqrt{A} < -\frac{2}{X_3}$. Let the numerator of $\mathrm{tr}(J(E_3))$ be $\mathrm{tr}_n(J_3)$, which can be rewritten as

$$\mathrm{tr}_n(J_3) = (AX_3^2 - 1)\,\mathrm{tr}_2 - X_3(2X_3 - 1 - E)(BX_3 + 2). \tag{15}$$

It is obvious that $\mathrm{tr}_n(J_3) < 0$ if $\mathrm{tr}_2 < 0$, indicating that $E_{3+}$ is AS when $\overline{X}_3 < X_{3+} < 1$.

For the case $X_3\sqrt{A} < 1$, the condition is reduced to $B > -2\sqrt{A}$, and $\mathrm{tr}_n(J_3)$ becomes

$$\begin{aligned} \mathrm{tr}_n(J_3) &< AX_3^2\,\mathrm{tr}_2 + 2\sqrt{A}X_3^2(2X_3 - 1 - E) - (X_3^2 - E) \\ &= (X_3\sqrt{A} - 1)\left(X_3^2 - E - \sqrt{A}X_3(3X_3^2 - 2(1 + E)X_3 + E)\right) < 0, \end{aligned} \tag{16}$$

because of

$$\begin{aligned} X_3^2 - E - \sqrt{A}X_3(-2(1 + E)X_3 + 3X_3^2 + E) &> X_3^2 - E - (3x_3^2 - 2(1 + E)X_3 + E) \\ &= 2(X_3 - 1)(-X_3 + E) > 0, \end{aligned}$$

under the assumption $\overline{X}_3 < X_{3+} < \min\{1, X_{SN}\}$. Summarizing the above discussions leads to the conclusion in (A) that $E_{3+}$ is AS for $\overline{X}_3 < X_{3+} < \min\{1, X_{SN}\}$.

It is known that $\mathrm{tr}_2 \geq 0$ for $X_{3+} \in (E, \overline{X}_3)$. Therefore, there are two possible cases:

(a) when $\mathrm{tr}_1 \geq 0$, except for $\mathrm{tr}_1 = \mathrm{tr}_2 = 0$, $E_{3+}$ is unstable;
(b) when $\mathrm{tr}_1 < 0$, $E_{3+}$ is AS (unstable) if $A < A_H$ ($A > A_H$), and Hopf bifurcation occurs at $A = A_H$,

where $\mathrm{tr}_1 = \mathrm{tr}_2 = 0$ defines a special Hopf critical point. $A_H$ denotes the Hopf critical point by considering $A$ as the bifurcation parameter such that $\mathrm{Tr}(J_3)|_{A=A_H} = 0$, given by

$$A_H(X_3) = \frac{\mathrm{tr}_1(X_3)}{-\mathrm{tr}_2(X_3)X_3^2}. \tag{17}$$

Further, to find the transversal condition of the Hopf bifurcation, we calculate the derivative of the trace on the equilibrium $E_{3+}$ at the critical point $A = A_H$ to obtain

$$T_{\mathrm{trans}} = \frac{1}{2}\left.\frac{\partial \mathrm{Tr}\,(J_3)}{\partial A}\right|_{A=A_H} = \frac{X_3^2(1 - X_3)(X_3 - E)(BX_3 + 2)}{2\left(A_H X_3^2 + BX_3 + 1\right)^2} \neq 0.$$

This implies that when $B > \max\{-2\sqrt{A}, -\frac{2}{X_3}\}$, Hopf bifurcation occurs from $E_{3+}$ at the critical point $A = A_H$. To consider the case (a), we first determine the sign of $\mathrm{tr}_1$ which is a cubic polynomial in $X_3$. Further, because its closed-form solution is inconvenient

to be used in the analysis, we try to get information from its values evaluated at $X_3 = E$ and $X_3 = 1$:

$$\begin{aligned} \mathrm{tr}_1|_{X_3=E} &= -E(E-1)(BE+1)\begin{cases} >0, & \text{for } B > -\frac{1}{E}, \\ \le 0, & \text{for } B \le -\frac{1}{E}, \end{cases} \\ \mathrm{tr}_1|_{X_3=1} &= (E-1)(B+1)\begin{cases} >0, & \text{for } B < -1, \\ \le 0, & \text{for } B \ge -1, \end{cases} \end{aligned} \tag{18}$$

as well as its derivatives:

$$\begin{aligned} \frac{\mathrm{dtr}_1}{\mathrm{d}X_3} &= -6BX_3^2 + 2((E+1)B-1)X_3, \\ \frac{\mathrm{d}^2\mathrm{tr}_1}{\mathrm{d}X_3^2} &= -12BX_3 - 2(1-B-BE). \end{aligned}$$

Since $-\frac{1}{E} < 1$, it is obvious that $\mathrm{tr}_1$ may have 1 or 3 roots in the interval $X_3 \in (E,1)$ if $-\frac{2}{E} < B \le -\frac{1}{E}$ or $B > -1$, and may have 0 or 2 roots in the interval $X_3 \in (E,1)$ if $-\frac{1}{E} < B < -1$.

When $-1 \le B < 0$, it is easy to show that the equation $\mathrm{tr}_1 = 0$ has only one real root in the interval $X_3 \in (E,1)$ because

$$\lim_{x\to-\infty} \mathrm{tr}_1 < 0, \quad \mathrm{tr}_1(X_3 = 0) = E, \quad \text{and} \quad \lim_{x\to+\infty} \mathrm{tr}_1 > 0. \tag{19}$$

Moreover, it is straightforward to determine that $\mathrm{tr}_1$ has two roots when $-\frac{1}{E} < B < -1$, according to (18) and the fact that at the midpoint of $E$ and 1, we have

$$\mathrm{tr}_1\big|_{X_3=\frac{1+E}{2}} = -\frac{(E-1)^2}{4} < 0.$$

To further determine the number of solutions for $B > 0$ and $-\frac{2}{E} < B \le -\frac{1}{E}$, we calculate the second derivatives of $\mathrm{tr}_1$ at the two critical points: $X_3 = 0$ and $X_3 = \frac{BE+B-1}{3B}$, at which $\frac{\mathrm{dtr}_1}{\mathrm{d}X_3} = 0$, to obtain

$$\begin{aligned} \left.\frac{\mathrm{d}^2\mathrm{tr}_1}{\mathrm{d}X_3^2}\right|_{X_3=0} &= 2(1-B-BE)\begin{cases} >0, & \text{for } B > \frac{1}{1+E}, \\ <0, & \text{for } B < \frac{1}{1+E}, \end{cases} \\ \left.\frac{\mathrm{d}^2\mathrm{tr}_1}{\mathrm{d}X_3^2}\right|_{X_3=\frac{BE+B-1}{3B}} &= 2\big[1-(E+1)B\big]\begin{cases} <0, & \text{for } B > \frac{1}{1+E}, \\ >0, & \text{for } B < \frac{1}{1+E}. \end{cases} \end{aligned}$$

This shows that $X_3 = 0$ and $X_3 = \frac{BE+B-1}{3B}$ are the local maximum point and local minimum point of the function $\mathrm{tr}_1$, respectively, when $B < \frac{1}{1+E}$. Moreover, note that $\frac{BE+B-1}{3B}$ is out of the interval that we consider ($\frac{BE+B-1}{3B} < E$) when $B \in (0, \frac{1}{1+E})$, since $-\frac{1}{2E-1} > \frac{1}{1+E}$ for $E \in (0, \frac{1}{2})$. Thus, the function $\mathrm{tr}_1$ has one real root when $B \in (0, \frac{1}{1+E})$. When $B > \frac{1}{1+E}$, $\mathrm{tr}_1$ has local minimum at $X_3 = 0$ as $\mathrm{tr}_1|_{X_3=0} = E$, leading to the same conclusion as that for $B \in (0, \frac{1}{1+E})$. The same conclusion can be drawn when $-\frac{2}{E} < B < -\frac{1}{E}$ by a similar argument.

Summarizing the above discussions, we have the following conclusion on the number of the roots of $\mathrm{tr}_1$:

$$\text{The number of real roots of } \mathrm{tr}_1 = \begin{cases} 1\text{: } X_{3a}, & \text{for } -\frac{2}{E} < B \le -\frac{1}{E} \text{ or } B \ge -1, \\ 2\text{: } X_{3a} \text{ and } X_{3b}, & \text{for } -\frac{1}{E} < B < -1. \end{cases} \tag{20}$$

In additiona, we have $\frac{\mathrm{dtr}_1}{\mathrm{d}X_3}|_{X_3=X_{3a}} < 0$ ($\frac{\mathrm{dtr}_1}{\mathrm{d}X_3}|_{X_3=X_{3a}} > 0$) for $B \ge 1$ ($\frac{2}{E} < B \le -\frac{1}{E}$). To clarify, we must compare $X_{3a}$ and $X_{3b}$ with $\overline{X}_3$ such that $X_3 < \overline{X}_3$ is satisfied, since it has been shown above that $\mathrm{E}_{3+}$ is AS for $X_3 > \overline{X}_3$.

To achieve this, we substitute $X_3 = \overline{X}_3$ into $\mathrm{tr}_1$ to obtain

$$\widetilde{\mathrm{tr}}_1 = \mathrm{tr}_1|_{X_3=\overline{X}_3} = \frac{P_1}{27}\left(B_2 - B\right), \quad \text{where} \quad P_1 = 2(1-E+E^2)^{\frac{3}{2}} + (1-2E)(2+E-E^2), \tag{21}$$

where $B_2$ is given in (9). It is easy to see that $P_1 > 0$ for $E \in (0, \frac{1}{2})$ and $\widetilde{\mathrm{tr}}_1 < 0$ if $B > B_2$. Consequently, $X_{3a} < \overline{X}_3$ only if $B > \max\{B_2, -\frac{1}{E}\}$. Hence, $\mathrm{E}_{3+}$ is unstable for $E < X_{3+} < X_{3a}$ if $B > \max\{B_2, -\frac{1}{E}\}$, which leads to the conclusion of the case (a). Similarly, it can be shown that $\overline{X}_3 < X_{3a}$ for the remaining case $B_2 < B < -\frac{1}{E}$ and $\mathrm{tr}_1 < 0$, for which the discussion on $\mathrm{tr}_1 < 0$ is given above. The stability analysis for case (b) has two subcases:

(b-1) $B > \max\{-\frac{1}{E}, B_2\}$, $X_{3a} < X_3 < \overline{X}_3$; and
(b-2) $B_2 < B < -\frac{1}{E}$, $E < X_3 < \overline{X}_3$.

We move on to show that Hopf bifurcation exists for these two cases. Using (17) with a direct calculation, we have that

$$A_{\mathrm{H}}(X_3 = X_{3a}) = 0, \quad \lim_{X_3 = \overline{X}_3} A_{\mathrm{H}} = +\infty, \quad A_{\mathrm{H}}\Big(X_3 = -\frac{2}{B}\Big) = \frac{B^2}{4},$$
$$\text{and} \quad A_{\mathrm{H}}(X_3 = E) = \frac{-(BE+1)}{E^2} \begin{cases} > 0, & \text{for } B < -\frac{1}{E}, \\ < 0, & \text{for } B > -\frac{1}{E}. \end{cases} \tag{22}$$

It is known that Hopf bifurcation exists at $A = A_{\mathrm{H}}$ for case (b). Moreover, one observes that the function $A_{\mathrm{H}}(X_3)$ takes values from the interval $(0, \infty)$ when the condition in (b-1) is satisfied. This implies that at least one Hopf bifurcation point exists for the condition in (b-1), since the equation $A = A_{\mathrm{H}}(X_3)$ must have solution in $X_3 \in (X_{3a}, \overline{X}_3)$.

Similarly, one can find $A > A_{\mathrm{H}}(X_3 = E)$ for the case (b-2) and $B < -\frac{1}{E} < -2$ since $E \in (0, \frac{1}{2})$. Note that the condition $B > -2\sqrt{A}$ is required to ensure that the model being biological meaningful, corresponding to $A > \frac{B^2}{4}$ for negative $B$. And a direct calculation gives the following relationship,

$$\frac{B^2}{4} - A_{\mathrm{H}}(X_3 = E) = \frac{(BE+2)^2}{4E^2} > 0,$$

which implies that $A = A_{\mathrm{H}}(X_3)$ has at least one root as the condition $B > -2\sqrt{A}$ holds. Therefore, Hopf bifurcation occurs from $\mathrm{E}_{3+}$ for case (b-2), provided that the condition $B > -2\sqrt{A}$ is satisfied.

Next, our goal is to identify the potential numbers of Hopf bifurcations and determine the stability conditions for the remaining conditions. Note that Hopf bifurcation exists at $A = A_{\mathrm{H}}$, where $A_{\mathrm{H}}$ is a function depending upon $X_3$, $B$ and $E$. If the parameters $B$ and $E$ are fixed, then there may exist multiple Hopf bifurcations if $A_{\mathrm{H}}$ is non-monotonic with respect to $X_3$. In this case, we first find the derivative of $A_{\mathrm{H}}$ with respect to $X_3$:

$$\frac{\mathrm{d}A_{\mathrm{H}}}{\mathrm{d}X_3} = \frac{g_2 \frac{\mathrm{d}\mathrm{tr}_1}{\mathrm{d}X_3} - \mathrm{tr}_1 \frac{\mathrm{d}g_2}{\mathrm{d}X_3}}{g_2^2}, \tag{23}$$

where $g_2 = -\mathrm{tr}_2(X_3)X_3^2$. Because the sign of $\frac{\mathrm{d}\mathrm{tr}_1}{\mathrm{d}X_3}$ and $\frac{\mathrm{d}g_2}{\mathrm{d}X_3}$ can be positive or negative as $X_3$ is varied, we rewrite the numerator of $\frac{\mathrm{d}A_{\mathrm{H}}}{\mathrm{d}X_3}$ as

$$g_2 \frac{\mathrm{d}\mathrm{tr}_1}{\mathrm{d}X_3} - \mathrm{tr}_1 \frac{\mathrm{d}g_2}{\mathrm{d}X_3} = 2X_3 G_3(X_3),$$

where

$$\begin{aligned} G_3(X_3) &= BG_1(X_3) + G_2(X_3), \\ G_1(X_3) &= X_3^3\left(3X_3^2 - (3E+3)X_3 + E^2 + E + 1\right), \\ G_2(X_3) &= 3X_3^4 - (E+1)X_3^3 - 6EX_3^2 + 3E(1+E)X_3 - E^2, \end{aligned} \tag{24}$$

for convenience in the analysis. Based on that, it is evident that the monotonicity of $A_{\mathrm{H}}(X_3)$ depends on the sign of $G_3(X_3)$. It is not possible to derive the analytic solution of $G_3(X_3)$ since it is a 5th-degree polynomial. Nonetheless, the subsequent discussion will help determine the number of solutions for $G_3(X_3) = 0$. By employing the discriminant of the quadratic polynomial factor of $G_1$, given by

$$\Delta_1 = 9(1+E)^2 - 12(E^2 + E + 1) = -3(1-E)^2 < 0,$$

we can conclude that $G_1 > 0$ for $E \in (0, \frac{1}{2})$.

For the quartic polynomial $G_2$, it can be shown that $G_2 = 0$ has two real solutions smaller than $E$ and out of the considered range because

$$\lim_{x \to -\infty} G_2 > 0, \quad G_2(0) = -E^2, \quad G_2(E) = 2E^2(1-E)^2, \quad G_2(1) = 2(1-E)^2.$$

$G_2 = 0$ may have either zero or two solutions in $X_3 \in (E, 1)$ due to $G_2(1) > 0$. The discriminant of $G_2$ is equal to

$$\Delta_2 = 108E^3(1-E)^2(E^4 - 92E^3 + 70E^2 - 92E + 1),$$

which yields a unique positive root $E_h^0 = 0.0109596\cdots$, implying that $G_2 = 0$ has two distinct real solutions, denoted by $X_3^1$ and $X_3^2$, for $0 < E < E_h^0$. Moreover, we have $G_2 < 0$ for $X \in (X_3^1, X_3^2)$, and $G_2 > 0$ for $X \notin (X_3^1, X_3^2)$. In addition, $G_2 > 0$ for $E_h^0 < E < \frac{1}{2}$. The above discussion leads to the following conclusion:

(1) When $E \in (0, E_h^0) \bigcup (E_h^0, \frac{1}{2})$ and $X_3 \in (E, X_3^1) \bigcup (X_3^2, \frac{1}{2})$, only negative values of $B$ can appear in the equation $\frac{\mathrm{d}A_{\mathrm{H}}}{\mathrm{d}X_3} = 0$.

(2) When $E \in (0, E_h^0)$, only positive values of $B$ can appear in $\frac{\mathrm{d}A_{\mathrm{H}}}{\mathrm{d}X_3} = 0$ for $X \in (X_3^1, X_3^2)$.

Based on the above findings, we calculate $G_3$ at some specific points, as shown in Table 1. The restriction $B > -\frac{2}{E}$ indicates that the two solutions of $G_3 = 0$ are less than $E$ and fallen outside the interval under consideration. Furthermore, it is found that another

**Table 1**
The function $G_3(X_3)$ and its derivatives at some special points.

| $X_3$ | $G_3(X_3)$ |
|---|---|
| $-\infty$ | $+\infty$ |
| 0 | $-E^2 < 0$ |
| $E$ | $E^2(E-1)^2(BE+2)\begin{cases} >0 & \text{for } B > -\frac{2}{E}, \\ =0 & \text{when } B = -\frac{2}{E}. \end{cases}$ |
| 1 | $(E-1)^2(B+2)\begin{cases} >0 & \text{for } B > -2, \\ =0 & \text{when } B = -2, \\ <0 & \text{for } B < -2. \end{cases}$ |
| $-\frac{2}{B}$ | $-\frac{(BE+2)\left(B^2E+(4E+4)B+12\right)(B+2)}{B^4}\begin{cases} \geq 0, & \text{for} B \in [B_2,-2), \\ <0, & \text{for} B \in \left(-\frac{2}{E}, B_2\right). \end{cases}$ |
| $+\infty$ | $-\infty$ |

real root of $G_3$ is out of the range (greater than 1) if $B > -2$. Similarly, for $B_2 < B < -2$, another real root of $G_3$ is in $X_3 \in (-\frac{2}{B}, 1)$. This implies that $G_3$ may have zero or two roots for $X_3 \in (E, \min\{-\frac{2}{B}, 1\})$ if $B > B_2$.

The number of solutions to $G_3 = 0$ can be further determined by eliminating $X_3$ from the equations $G_3 = 0$ and $\frac{\mathrm{d}G_3}{\mathrm{d}X_3} = 0$, giving the following resultant: $\mathrm{Res} = E(E-1)R_1R_2$, where

$$\begin{aligned} R_1 = {} & B^4E^8 + 4B^4E^7 + 10B^4E^6 - 4B^3E^7 + 16B^4E^5 + 8B^3E^6 + 19B^4E^4 + 164B^3E^5 + 6B^2E^6 \\ & + 16B^4E^3 + 68B^3E^4 - 120B^2E^5 + 10B^4E^2 + 68B^3E^3 + 1008B^2E^4 - 4BE^5 + 4B^4E + 164B^3E^2 \\ & - 900B^2E^3 + 200BE^4 + B^4 + 8B^3E + 1008B^2E^2 + 44BE^3 + E^4 - 4B^3 - 120B^2E + 44BE^2 \\ & - 92E^3 + 6B^2 + 200BE + 70E^2 - 4B - 92E + 1, \\ R_2 = {} & B^2E + 4BE + 4B + 12. \end{aligned} \tag{25}$$

Solving $R_2 = 0$ gives the solution $B = B_2 < -2$. Furthermore, it is observed that the graph $G_3(X)$ intersects the $X$-axis at $X_3 = \overline{X}_3$ when $B = B_2$. At this special point, $\det(J(\mathrm{E}_3)) = \mathrm{tr}(J(\mathrm{E}_3)) = 0$, leading to a B-T bifurcation occurring at $X_3 = \overline{X}_3$ if $B = B_2$. The other intersection points can be found by solving $R_1 = 0$. However, solving the high-degree polynomial $R_1$ in $B$ and $E$ explicitly is not possible. Hence, we denote $B_1$ as the solution to the implicit function $R_1 = 0$, and the intersection point is denoted by $\widetilde{X}_3$. Then, finding the discriminant of $R_1$ for $B$, we have

$$\Delta_3 = -268435456E^7(1-E)^6(9E^2-7E+9)^2(81E^6+54E^5-9E^4+232E^3-9E^2+54E+81)^2 < 0,$$

implying that $R_1 = 0$ has only two real solutions $B_{1a}$ and $B_{1b}$. In addition, it can be shown that the two solutions satisfy that $0 < B_{1a} < B_{1b}$ if $0 < E < E_h^0$, and $B_{1a} < 0 < B_{1b}$ if $E_h^0 < E < \frac{1}{2}$. From the conditions in (1), we know that only negative values of $B$ can appear in $G_3 = 0$, implying that $G_3(X)$ intersects the $X$-axis when $B = B_{1a}$ if $E_h^0 < E < \frac{1}{2}$. Therefore, we will use the notation $B_1 = B_{1a}$ in the following for the convenience of analysis. Let the corresponding intersection point be $\widetilde{X}_3$. To compare $B_1$ with $B_2$, we substitute $B = B_2$ into $R_1$, which yields $R_1 > 0$ for $E \in (0, \frac{1}{2})$, implying that the intersection point $\widetilde{X}_3 < \overline{X}_3$. Additionally, $B_1$ and $B_2$ cannot take the same value simultaneously within the range $0 < E < \frac{1}{2}$ because the two equations $R_1 = R_2 = 0$ do not have a solution for $(B, E)$ under the condition on $E$. Using a graphical approach to plot the implicit function $R_1$ and $R_2$ on the $B$-$E$ plane, one can show that $B_1 > B_2$.

Besides, calculating the second derivatives of $G_3$ at $B = B_2$, $X_3 = \overline{X}_3$, we obtain

$$\left.\frac{d^2G_3}{dX_3^2}\right|_{B=B_2, X_3=\overline{X}_3} = \frac{1}{3}\left[(10E+10)\sqrt{E^2-E+1} - 26E^2 + 32E - 26\right] < 0, \quad \text{for} \quad E \in \left(0, \frac{1}{2}\right).$$

This shows that $G_3(X_3)$ is concave downward at $X_3 = \overline{X}_3$ when $B = B_2$ and concave upward at $X_3 = \widetilde{X}_3$. Hence, based on this result for (24), we know that as $B$ decreases, the curve of $G_3$ touches the $X_3$-axis first at $X_3 = \widetilde{X}_3$ when $B = B_1$ and then at $X_3 = \overline{X}_3$ when $B = B_2$. $G_3 > 0$ for $X_3 \in (E, \min\{-\frac{2}{B}, 1\})$ if $B > B_1$ and $G_3$ has two solutions in the given range if $B_2 < B < B_1$.

Summarizing the above discussions, we conclude that $A_{\mathrm{H}}$ increases monotonically for both cases (b-1) and (b-2) if $B > B_1$ based on (22), since $G_3 > 0$ $\left(\frac{\mathrm{d}A_{\mathrm{H}}(X_3)}{\mathrm{d}X_3} > 0\right)$ in the range under consideration. Therefore, $A = A_{\mathrm{H}}(X_3)$ can have only one solution in $X_3 \in (E, \overline{X}_3)$, which corresponds to the unique Hopf bifurcation point $\mathrm{E}_{\mathrm{H}_1}$. Moreover, for both cases (b-1) and (b-2), we have $A > A_{\mathrm{H}}$ for $X_3 \in (E, X_{\mathrm{H}_1})$. Combining these results with the conclusion for case (a), as well as the previous argument that $X_3$ is monotonically decreasing as $C$ increases on $\mathrm{E}_{3+}$, we know that under the condition (A-1), $X_3$ is unstable for $C \in (C_{\mathrm{H}_1}, C_E)$, and asymptotically stable for $C \in (C_{\mathrm{SN}}, C_{\mathrm{H}_1})$,

When $B \in (B_2, B_1)$, it is noted that $G_3 = 0$ has two real solutions $X_M$ and $X_m$, at which $A_{\mathrm{H}}(X_3)$ gets its local maximum and local minimum, respectively. Therefore, $A = A_{\mathrm{H}}(X_3)$ can have three real solutions if $A$ satisfies $A_{\mathrm{H}}^m < A < A_{\mathrm{H}}^M$, leading to the three corresponding Hopf bifurcation points. Further, it follows from (22) that $A > A_{\mathrm{H}}$ (resp. $A < A_{\mathrm{H}}$) for $X_3 \in (E, X_{\mathrm{H}_3}) \bigcup (X_{\mathrm{H}_2}, X_{\mathrm{H}_1})$

(resp. $X_3 \in (X_{H_3}, X_{H_2}) \bigcup (X_{H_1}, \overline{X}_3)$). Thus, the conclusion on the stability can be drawn for the case (A-2)(b) in Theorem 2. Otherwise, only one Hopf bifurcation exists for the remaining case (A-2)(a). Because $A > A_H$ when $X_3 \in (E, X_{H_1})$ for the case (A-2)(a), it has the same stability conclusion as that for the case (A-1).

**Case 2:** $\max\{-2\sqrt{A}, -\frac{2}{E}\} < B \le B_2$. Now, we turn to consider the case $B < B_2$. First, it follows from (20) that $\mathrm{tr}_1 = 0$ has one solution $X_{3a}$ when $B < \min\{B_2, -\frac{1}{E}\}$. When $E < \frac{3}{8}$, $\mathrm{tr}_1 = 0$ has two solutions in $X_3 \in (E, 1)$ if $-\frac{1}{E} < B < B_2$, but only one solution in $X_3 \in (E, X_{SN})$, since

$$\mathrm{tr}_1\big|_{X_3 = X_{SN}} = \frac{B^2 E + 4B(E+1) + 12}{B^2} < 0, \quad \text{for} \quad B < B_2.$$

Further, we find $\widetilde{\mathrm{tr}}_1 < 0$ for $\max\{-2\sqrt{A}, -\frac{2}{E}\} < B < \min\{B_2, -\frac{1}{E}\}$. Thus, if $\max\{-\frac{1}{E}, -2\sqrt{A}\} < B < B_2$, $E_{3+}$ is unstable for $E < X_{3+} < X_{3a}$, and the stability of $E_{3+}$ for the remaining cases depends on the function $A_H(X_3)$, which follows the conditions in (b). Because $G_3(X_3)$ gets its local maximum at $X_3 = \overline{X}_3$ when $B = B_2$, and it is decreasing as $B$ is decreasing, $G_3$ has a unique root for $-2\sqrt{A} < B < B_2$, which is smaller than $\widetilde{X}_3$. Note that for this case, $\overline{X}_3 > X_{SN}$. Therefore, when $A > A_H^M$, no Hopf bifurcations can occur for this case and $E_{3+}$ is unstable, which is the case (B-1). Otherwise, $A = A_H(X_3)$ has two solutions, yielding two Hopf bifurcation points at $X_3 = X_{H_1}$ and $X_3 = X_{H_2}$. Then, $A > A_H$ (resp. $A < A_H$) for $X_3 \in (E, X_{H_2}) \bigcup (X_{H_1}, X_{SN})$ (resp. $X_3 \in (X_{H_2}, X_{H_1})$), leading to the conclusion on the stability for the case (B-2) in Theorem 2.

The proof for Theorem 2 is finished. □

The above analysis shows that for certain parameter values, the system (3) can exhibit multistable states. Note that the equilibrium $E_0$ remains stable. Further, it will be shown in the simulation part (next section) that the Hopf bifurcation can have codimension two when the Hopf bifurcation is subcritical. Thus, it is possible to have an outer stable limit cycle surrounding an unstable small limit cycle, and both of them enclose a stable $E_3$. In this case, we reach a tetrastable state if $E_1$ is also stable. We will further show this by simulations in the next section, where we will first determine the conditions which yield at least tristablity.

We define two types of multistable phenomena: Type-I multistable states representing the coexistence of stable equilibria; and Type-II multistable states involving stable equilibria and stable limit cycles. In the following discussions, the lower multistable states are not included when we discuss a higher multistable state. For example, the tetrastable state excludes the bistable and tristable states. The conditions for bistable states are easy to determine. If $B > -2$, only $E_0$ and $E_1$ are stable when $C < C_t$ and $X_3$ does not exist under this condition, while when $C > C_t$, bistable state occurs between $E_0$ and $E_3$ if the stability condition in Theorem 2 is satisfied. Regarding the higher multistable phenomena, we have the following theorem.

**Theorem 3.** *For system (3), no tristable states exist if $B \ge -2$ or when the condition* (B-1) *is held. Tyep-I tristable states exist, i.e., the three stable equilibria $E_0, E_1$ and $E_{3+}$ coexist,*

(i) *if $\max\{B_2, -2\sqrt{A}\} < B < -2$ when $C_{SN} < C < \min\{C_{H_1}, C_t\}$; or when the condition* (A-2)(b) *is held with the extra condition $C_{H_2} < C < \min\{C_{H_3}, C_t\}$ to be satisfied;*

(ii) *if the condition* (B-2) *holds together with the condition $C_{H_1} < C < \min\{C_{H_2}, C_t\}$ to be satisfied.*

*Type-II tristable states, including the stable $E_1$ and a stable limit cycle surrounding $E_{3+}$ exist, if $v_1 < 0$ and one of the following conditions holds:*

(I) (A-1) *or* (A-2)(a) *with $B < B_s$ and $A > A_H(X_t)$;*

(II) (A-2)(b) *with $B < B_s$ and $A > A_H(X_t)$;*

(III) (A-2)(b) *with $B < B_s$, $A < A_H(X_t)$ and $E > E_t^*$ or $E < E_t^*$, $G_3(X_3 = X_t) < 0$;*

(IV) (B-2) *with $A < \min\{A_H(X_t), A_H^M\}$.*

*No Type-II tristability exists for the case:*

(V) *when the condition* (B-2) *and $A > A_H(X_t)$ hold.*

*Here, the first focus value is given by*

$$v_1 = -\frac{v_{1a}}{8(-3X_3^2 + 2(1+E)X_3 - E)(BX_3 + 2)X_3}, \quad \text{where} \quad v_{1a} = C_2 B^2 + C_1 B + C_0, \tag{26}$$

*with*

$$C_2 = X^3(12X_3^5 - 9(E+1)X_3^4 + 2(E^2 + E + 1)),$$
$$C_1 = 39X_3^4 - 26(E+1)X_3^3 + 6(E^2+1)X_3^2 + E^2,$$
$$C_0 = (E - 4X_3 + 1)(E - X_3^2).$$

**Proof.** The conditions for the Type-I tristable phenomenon are easy to find, since the stability conditions for $E_1$ and $E_3$ have been explicitly obtained. We know that $E_0$ is always asymptotically stable and $E_1$ is stable for $C < C_t$, and the type-I tristable phenomenon can exist only if $E_{3+}$ is also stable. This requires the condition $C_{SN} < C_t$, leading to the constraint $B < -2$. Combining this with the stability conditions in Theorem 2, we find that if there is one Hopf bifurcation point in the cases (A-1) and (A-2)(a), $E_1$ and $E_3$ are both stable for $C \in (C_{SN}, \min\{C_{H_1}, C_t\})$. When there exist three Hopf bifurcations under the condition (A-2)(b), the Type-I

tristable states again occur for $C \in (C_{SN}, \min\{C_{H_1}, C_t\})$, but can also occur for $C \in (C_{H_2}, \min\{C_{H_3}, C_t\})$ if $C_{H_2} < C_t$. Similarly, when the condition (B-2) holds, the Type-I tristable states can only exist if $C_{H_1} < C < \min\{C_{H_2}, C_t\}$ is satisfied. Moreover, it is obvious that no tristable phenomenon can occur under the condition (B-1) since $E_{3+}$ is unstable.

It is more interesting to study the Type-II tristable phenomenon, for which $E_0$ and $E_1$ are stable, together with a stable periodic motion. Due to the existence condition $C_{SN} < C_t$ for $E_{3+}$, we only need to consider $B \in (\max\{-2\sqrt{A}, -\frac{2}{E}\}, -2)$. If there exist parameter values satisfying $\mathrm{tr}(J_3)|_{C=C_{SN}}\,\mathrm{tr}(J_3)|_{C=C_t} < 0$, then it is possible to have either one or three Hopf bifurcations, which may exist in the interval $C \in (C_{SN}, C_t)$. On the other hand, if $\mathrm{tr}(J_3)|_{C=C_{SN}}\,\mathrm{tr}(J_3)|_{C=C_t} > 0$, then either no Hopf bifurcation or two Hopf bifurcations might exist in the interval $C \in (C_{SN}, C_t)$. Note that only if at least one Hopf bifurcation exists in the range, then there is a possibility of having stable limit cycles. Moreover, tetrastable phenomenon is possible if the parameters satisfy the condition under which the Hopf bifurcation has codimension two. We leave it to be discussed in the next section.

Now, we assess the signs of $\mathrm{tr}(J_3)|_{C=C_{SN}}$ and $\mathrm{tr}(J_3)|_{C=C_t}$. A direct computation gives

$$\mathrm{tr}(J_3)|_{C=C_{SN}} = \frac{B^2-4A}{B^4}(EB^2+4(1+E)B+12)\begin{cases} <0, & \text{if } B \in \big(\max\{-2\sqrt{A}, B_2\}, -2\big),\\ =0, & \text{if } B = B_2,\\ >0, & \text{if } B \in \big(-\frac{2}{E}, B_2\big).\end{cases} \tag{27}$$

Because $\mathrm{tr}(J_3)|_{C=C_{SN}}$ changes its sign at $B = B_2$, the following discussions will be divided into two cases: $B > B_2$ and $B < B_2$, which are actually the cases (A) and (B) in Theorem 2. Recall the conclusion in Theorem 2 that $E_{3+}$ remains stable within the interval $X_3 \in (\overline{X}_3, X_{SN})$ for the case (A). Further, it is determined that $F_1 = 0$ has two solutions $X_3 = X_1 = 1$ and $X_3 = X_t = -\frac{1}{B+1}$ at $C = C_t$. To determine the sign of $\mathrm{tr}(J_3)|_{C=C_t}$, we substitute the second solution $X_3 = X_t$ into $\mathrm{tr}(J_3)$. Therefore, for $X_t \in (\overline{X}_3, X_{SN})$, it is clear that no Hopf bifurcation can occur in $C \in (C_{SN}, C_t)$ and $E_3$ remains asymptotically stable in this given range and no Type-II tristable can occur. Thus, the existence of the Type-II tristable states requires the additional condition $X_t < \overline{X}_3$, which is guaranteed under the restriction,

$$B < B_s = \frac{-2E+\sqrt{E^2-E+1}-1}{E}.$$

Under these conditions, we have $\mathrm{tr}(J_3)|_{C=C_t} > 0$ if $A > A_H(X_3 = X_t)$, which directly gives the following conclusion when the condition for case (A) is satisfied:

$$\mathrm{tr}(J_3)|_{C=C_{SN}}\,\mathrm{tr}(J_3)|_{C=C_t}\begin{cases} >0, & \text{if } A < A_H(X_3 = X_t),\\ <0, & \text{if } A > A_H(X_3 = X_t).\end{cases} \tag{28}$$

Since there is only one Hopf bifurcation under the condition (A-1) or (A-2)(a), the Type-II tristable phenomenon can only occur for these two cases if $\mathrm{tr}(J_3)|_{C=C_{SN}}\,\mathrm{tr}(J_3)|_{C=C_t} < 0$ and $X_{H_1} \in (X_t, X_{SN})$, which in turn requires $A > \max\{A_H(X_3 = X_t), \frac{B^2}{4}\}$. Otherwise, no Hopf bifurcation can exist in $C \in (C_{SN}, C_t)$ and so no Type-II tristable states exist for the cases (A-1) and (A-2)(a). The condition (I) is proved.

For the condition (A-2)(b), three Hopf bifurcations may exist. However, one cannot determine the possibility of the Type-II tristable state merely based on the sign of $\mathrm{tr}(J_3)|_{C=C_{SN}}\,\mathrm{tr}(J_3)|_{C=C_t}$ because there are possibilities of having multiple or zero Hopf bifurcation points located in the interval $X_3 \in (X_t, X_{SN})$. Thus, in order to determine the number of Hopf critical points in the considered interval, we need to compare $X_t$ with $X_M$ and $X_m$, since it leads to the comparison of $X_H$ with $X_t$. We first calculate $G_3$ at $X_3 = X_t$ to obtain

$$G_3(X_3 = X_t) = \frac{(B+2)}{(1+B)^5}F_2,$$

where

$$F_2 = -\big[B^4E^2 + 3(2E^2+E)B^3 + (11E^2+13E+1)B^2 + 2(4E^2+7E+1)B + 2(E^2+2E-1)\big].$$

It has been proved for Theorem 2 that $G_3$ has two roots $X_3 = X_M$ and $X_3 = X_m$ in the interval $X_3 \in (E, \overline{X}_3)$ for the case (A-2)(b). Also, it is clear from the above discussion that $X_t \in (X_M, X_m)$ if $G_3(X_3 = X_t) < 0$.

However, there are two possibilities for $G_3(X_3 = X_t) > 0$: $X_t < X_M$ and $X_t > X_m$. To further determine the position of $X_t$, we eliminate $X_t$ from the two equations: $G_3(X_3 = X_t) = 0$ and $\frac{dG_3}{dX_3}(X_3 = X_t) = 0$, giving the resultant:

$$\mathrm{Res}_t = (E^6 + 15E^5 + 84E^4 - 115E^3 + 141E^2 - 42E + 1)(E-1).$$

Solving $\mathrm{Res}_t = 0$ for $E$, under the constraint $E \in (0, \frac{1}{2})$, we find the parameter values,

$$(B, E) = (B_t^*, E_t^*) = (-2.579834\cdots, 0.350565\cdots),$$

at which $G_3$ intersects the $X$-axis at $X_3 = X_t$. Therefore, we have

$$X_t > X_m, \quad \big(\tfrac{dG_3}{dX_3}(X_3 = X_t) > 0\big), \quad \text{if } E < E_t^*,$$
$$X_t < X_M, \quad \big(\tfrac{dG_3}{dX_3}(X_3 = X_t) < 0\big), \quad \text{if } E > E_t^*.$$

This gives the conditions for the position of $X_t$, which determines the number of Hopf bifurcation points in $C \in (C_{SN}, C_t)$. To further study the stability of the bifurcating limit cycles, we apply the method of normal forms associated with Hopf and generalized Hopf

bifurcations, and the Maple program [26] to obtain the first-order focus value $v_1$ given in (26). Then, if $v_1 < 0$ (resp. $v_1 > 0$), the Hopf bifurcation is supercritical (resp. subcritical) and the bifurcating limit cycle is stable (resp. unstable) enclosing an unstable (resp. a stable) focus.

Combining the above results with the formula $v_1$ given in (26), we obtain the following conclusions, corresponding to the cases (II) and (III).

- When the condition (A-2)(b) with $A < A_{\rm H}(X_{\rm t})$ holds, then
  - either no Type-II tristable states exist if $G_3(X_3 = X_{\rm t}) > 0$ and $E < E_{\rm t}^*$;
  - or two Hopf critical points exist within $C \in (C_{\rm SN}, C_{\rm t})$ if $G_3(X_3 = X_{\rm t}) < 0$ or $G_3(X_3 = X_{\rm t}) > 0$, and $E > E_{\rm t}^*$, for which tristable states exist if $v_1 < 0$.
- When the condition (A-2)(b) with $A > A_H(X_{\rm t})$ holds, then
  - either one Hopf critical point exists for $C \in (C_{\rm SN}, C_{\rm t})$ if $G_3(X_3 = X_{\rm t}) < 0$ or $G_3(X_3 = X_{\rm t}) > 0$, and $E < E_{\rm t}^*$;
  - or three Hopf critical points exist within $C \in (C_{\rm SN}, C_{\rm t})$ if $G_3(X_3 = X_{\rm t}) > 0$ and $E > E_{\rm t}^*$;

  for which tristable states exist if $v_1 < 0$.

Having discussed the Type-II tristable phenomenon for the case (A), we now turn to consider the possibility of the Type-II tristable phenomenon for the case (B) when $B < B_2$. First, note that no tristable phenomenon can happen under the condition (B-1), because $\rm E_{3+}$ is unstable. Thus, we only need to consider the tristability for the case (B-2). Based on (27), a similar argument as that used in the above discussion can be applied to obtain that $\mathrm{tr}(J_3)|_{C=C_{\rm SN}}\,\mathrm{tr}(J_3)|_{C=C_{\rm t}} < 0$ if $A < A_{\rm H}(X_{\rm t})$. This implies that one Hopf bifurcation appears from $\rm E_{3+}$ at $C_{\rm H_1} \in (C_{\rm SN}, C_{\rm t})$.

On the other hand, $\mathrm{tr}(J_3)|_{C=C_{\rm SN}}\,\mathrm{tr}(J_3)|_{C=C_{\rm t}} > 0$ if $A > A_{\rm H}(X_{\rm t})$. So, either no Hopf bifurcation point or two Hopf bifurcation points exist in $(C_{\rm SN}, C_{\rm t})$ for $A > A_{\rm H}(X_{\rm t})$. Moreover, it is known that $G_3$ has a unique root and continues to decrease for $B < B_2$. Hence, for the case $A > A_{\rm H}(X_{\rm t})$ when (B-2) holds, it is clear that no Hopf bifurcation points exist in $(C_{\rm SN}, C_{\rm t})$ if $G_3(X_3 = X_{\rm t}) < 0$; whereas if $G_3(X_3 = X_{\rm t}) > 0$, two Hopf bifurcation points exist in the given range. In particular, we have found that codimension-two Hopf bifurcation cannot occur under the condition (B-2). Moreover, it is not possible to have $v_1 < 0$ at the Hopf bifurcation point if $A > A_{\rm H}(X_{\rm t})$ by searching for values in a given numerical range. This implies that no stable limit cycles exist and so no Type-II tristable states can occur for the case (V). But it is possible to obtain $v_1 < 0$ for the remaining case (IV) with $A < \min\{A_{\rm H}^M, A_{\rm H}(X_{\rm t})\}$, which will be discussed in the next section.

The existence of tetrastable is again based on the existence of Hopf bifurcation for $C \in (C_{\rm SN}, C_{\rm t})$, but it requires the existence of codimension-two Hopf bifurcation, namely, by normal form theory, it requires that the first and second focus values satisfy $v_1 = 0$ and $v_2 \neq 0$. This will be further discussed in the next section.

The proof of Theorem 3 is complete. □

## 4. Simulations

In this section, we present simulations to demonstrate the theoretical results obtained in the previous sections, particularly on Hopf bifurcation and the multistable phenomena, which agree with the bifurcation diagrams. The simulated examples are chosen from the following cases representing the multistable states:

- bistable state: case (A-1);
- tristable state: cases (I), (IV) and (V);
- tetrastable state: case (II),

as shown in Figs. 2–6. Some interesting phenomena can be observed such as more than one limit cycles bifurcating from a single Hopf critical point.

First, we show a bifurcation diagram, as depicted in Fig. 2, by taking parameter values for the case (A-1) in Theorem 2: $A = D = 1$, $B = -1$ and $E = \frac{3}{10}$. The bifurcation diagram projected on the $C$-$X$ plane is shown in Fig. 2(a), while the bifurcation diagram in the 3-d $C$-$X$-$Y$ space is given in Fig. 2(b), from which the bistability can be clearly observed between $\rm E_0$ and $\rm E_1$ for $C < C_{\rm t}$, and between $\rm E_0$ and $\rm E_{3+}$ for $C > C_{\rm t}$. It is seen that the positive (interior) solution of system (3) exists when the population of predators remains at a relatively small amount. At the above set of parameter values, we have a Hopf bifurcation from the equilibrium $\rm E_{3+} = (X_{3+}, Y_{3+}) \approx (0.556287, 0.153965)$ at the critical point $C_{\rm H_1} \approx 2.433852$, at which the first focus value is obtained as $v_1 \approx -0.014168 < 0$, indicating that the Hopf bifurcation is supercritical, agree with the bifurcation diagram.

The second example is chosen for the case (I) in Theorem 3, for which both Type-I and Type-II tristable phenomena exist. We choose parameter values: $D = 1$ and $E = 0.3$, for which

$$B_1 \approx -2.563933, \quad B_2 \approx -2.741204, \quad B_{\rm s} \approx -2.370601.$$

To ensure the conditions $B_1 < B < B_{\rm s}$ and $B > -2\sqrt{A}$, we take the values, $B = -2.5$ and $A = 3$, which yield that $C_{\rm SN} < C_{\rm H_1} < C_{\rm t}$, and the Hopf bifurcation occurs from the equilibrium $\rm E_{3+} = (X_3, Y_3) \approx (0.707701, 0.123476)$ at the critical point $C_{\rm H_1} \approx 1.464078$. Three values of $C$ are taken for simulations: (i) $C = 1.45$, for which the Type-I tristable states exist as all the three equilibria $\rm E_0$, $\rm E_1$ and

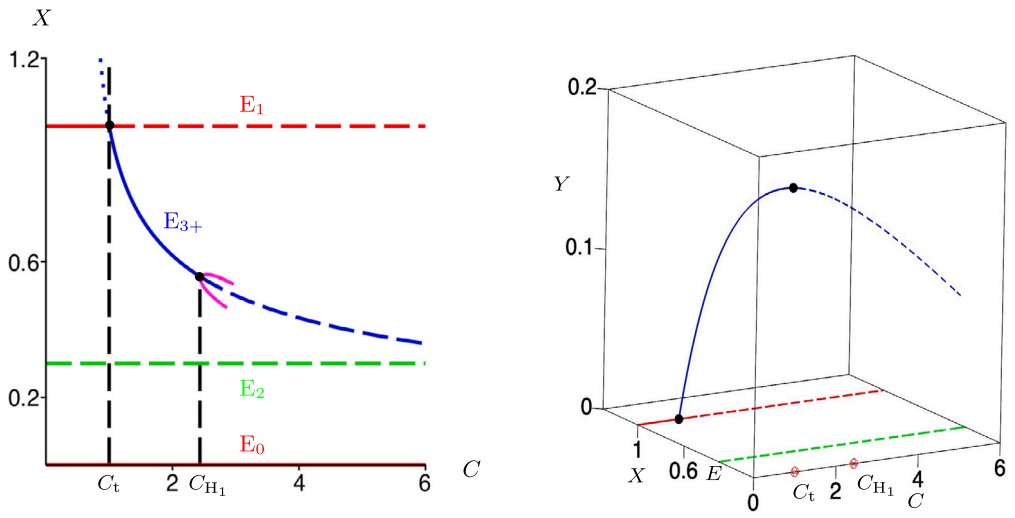


**Fig. 2.** Bifurcation diagrams of system (3) for $A = D = 1$, $B = -1$, $E = 0.3$: (a) projected on the $C$-$X_3$ plane; and (b) projected in the $C$-$X$-$Y$ space.

$E_{3+}$ are AS. (ii) $C = 1.48$ for which $E_1$ is AS while $E_{3+}$ is an unstable focus surrounded by a stable limit cycle. (iii) $C = 1.55$ for which $C > C_t$, implying that both $E_1$ and $E_{3+}$ are unstable, and $E_{3-}$ does not exist, but a stable limit cycle exists around $E_{3+}$. At this Hopf critical point, the first focus value equals $v_1 \approx -1.108573$, implying that the Hopf bifurcation is supercritical. The bifurcation diagram is shown in Fig. 3(a) and simulations are given in Fig. 3(b)–(d), which validate the theoretical predictions. Note that the notations $\Omega_{E_0}$, $\Omega_{E_1}$, $\Omega_{E_{3+}}$ and $\Omega_{LC_s}$ in Fig. 3(b) and (c) denote the trapping regions (attracting basins) for $E_0$, $E_1$, $E_{3+}$ and the stable limit cycle $LC_s$, respectively. They are separated by the blue curves $S_1$ and $S_{3-}$ which are the stable manifolds connecting the saddles $E_2$ and $E_{3-}$, respectively.

Another example showing the tristable states is depicted in Fig. 4 by taking the parameter values for the case (V) in Theorem 3. To satisfy the condition of this case, we first choose $E = 0.3$, yielding $B_2 \approx -2.741204$. We then take a value for $B = -4 < B_2$, which gives

$$A_H^M \approx 4.338853, \quad A_H(X_1) \approx 3.571429, \quad \frac{B^2}{4} = 4.$$

Further, we take $A = 4.3 < A_H^M$, which results in two Hopf bifurcation points defined by

$$C_{H_1} \approx 0.614483, \quad E_{3H_1} \approx (0.390505, 0.013237),$$
$$C_{H_2} \approx 0.379446, \quad E_{3H_2} \approx (0.438239, 0.012913).$$

It can be shown that $v_1 > 0$ for both the two Hopf bifurcations, implying that both the two Hopf bifurcations are subcritical, see the bifurcation diagram in Fig. 4(a). This indicates that the bifurcating limit cycles are unstable, as confirmed by the simulations depicted in Fig. 4(b) and (c). In Fig. 4(c), two initial points are chosen, denoted by the two blue points, to simulate the unstable limit cycle. Backward time integration is used to obtain the red and green colored trajectories, both converging to the unstable limit cycle. This clearly indicates that for this case, there does not exist Type-II tristable phenomenon since no stable limit cycles bifurcate from the Hopf bifurcation point, but the Type-I tristable states do exist.

However, the Type-II tristable phenomenon can also exist for the case (B-2). To achieve this, we must find possible parameter values such that $v_1 < 0$. By searching the values of $E \in (0, 0.5)$ with a step 0.01, and then searching the values of $B \in (-\frac{2}{E}, B_2)$ with a step 0.1, we obtain 7 sets of solutions satisfying $\frac{B^2}{4} < A < A_H^M$ to yield $v_1 < 0$. Moreover, all these 7 sets of solutions also satisfy $C_{SN} < C_{H_1} < C_t < C_{H_2}$, indicating that $E_3$ has only one Hopf bifurcation falling in the range that $E_1$ is AS, corresponding to the case (IV) in Theorem 3. Moreover, we do not find parameter values satisfying $v_1 = 0$ for the case (B-2), implying that most likely there do not exist parameter values which yield codimension-two Hopf bifurcation, and the number of bifurcating limit cycles is one. As an example, we take one of the 7 sets of solutions:

$$A = 2.8025, \quad B = -2.9, \quad D = 1, \quad E = 0.16.$$

Note that all the conditions listed for the case (IV) in Theorem 3 are satisfied and one can determine the two Hopf bifurcation points as

$$C_{H_1} \approx 0.725118, \quad E_{3H_1} \approx (0.621703, 0.078738),$$
$$C_{H_2} \approx 5.092997, \quad E_{3H_2} \approx (0.282012, 0.125823).$$

A direct computation yields

$$v_1(E_{3H_1}) \approx -0.007294, \quad v_1(E_{3H_2}) \approx 0.234366,$$

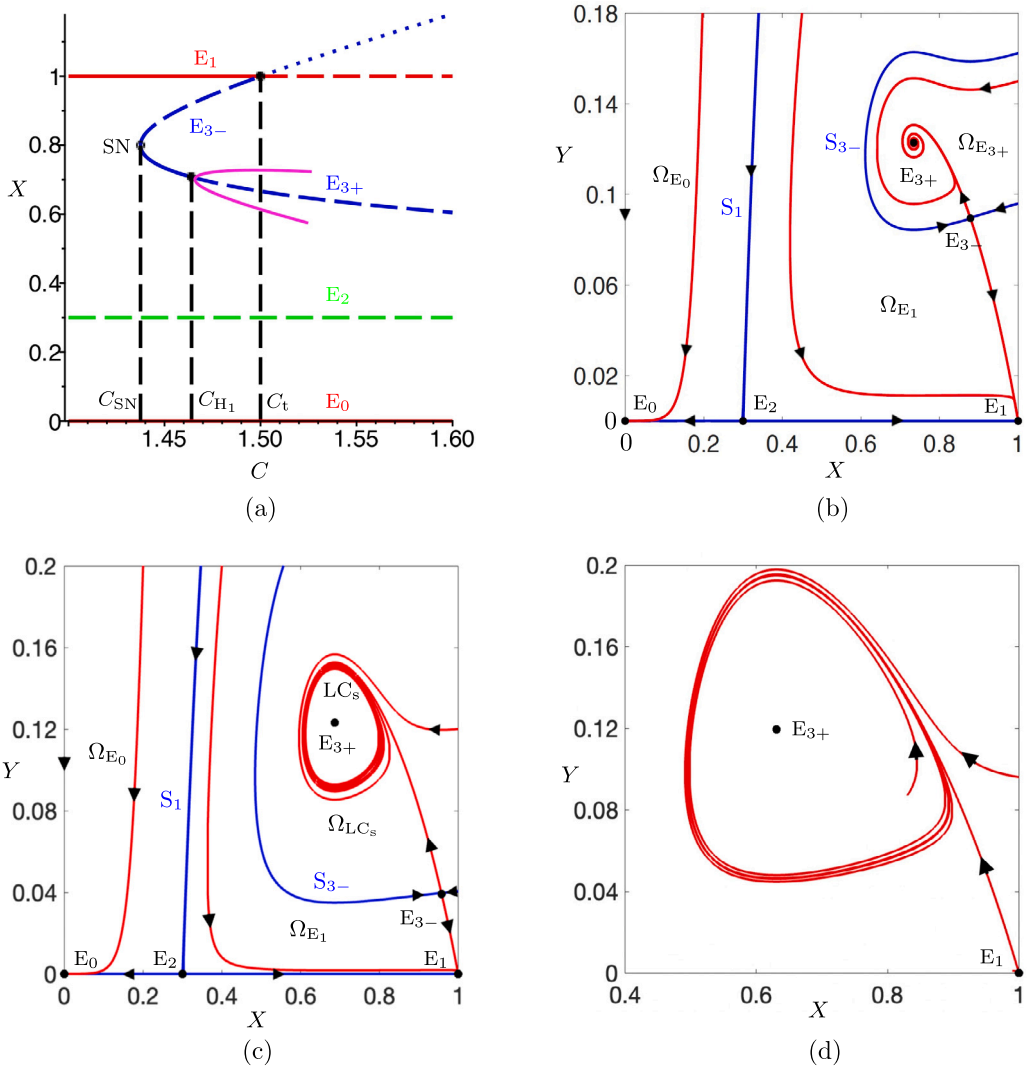


**Fig. 3.** Bifurcation diagram and simulations of system (3) for $A = 3$, $B = -2.5$, $D = 1$, $E = 0.3$: (a) bifurcation diagram projected on the $C$-$X$ plane, where solid and dashed curves represent stable and unstable equilibria, respectively; (b) simulated phase portrait for $C = 1.45$; (c) simulated phase portrait for $C = 1.48$; and (d) simulated phase portrait for $C = 1.55$.

indicating that the Hopf bifurcation is supercritical (subcritical) at $E_{3H_1}$ ($E_{3H_2}$), which can be seen from the bifurcation diagram in Fig. 5(a) and (b), where the pink solid (dashed) curve represents the stable (unstable) limit cycle. The Type-II tristable phenomenon also exists for $C \in (C_{SN}, C_{H_1})$ and the Type-I tristable state exists for $C \in (C_{H_1}, C_t)$. Two values of $C = 0.72$ and $C = 5$ are chosen for simulations: showing a stable limit cycle bifurcating from the supercritical Hopf bifurcation point $C_{H_1}$ (see Fig. 5(c)), yielding the Type-II tristable phenomenon (the AS $E_0$ is not shown in Fig. 5(c)); and an unstable limit cycle bifurcating from the subcritical Hopf bifurcation point $C_{H_2}$, leading to the Type-I bistable phenomenon with both $E_0$ and $E_3$ AS (see Fig. 5(e)).

The next example is chosen for the case (II) in Theorem 3, for which the system has three Hopf bifurcations, and both the tristable and tetrastable phenomena exist, with the parameters satisfying $C_{SN} < C_{H_1} < C_{H_2} < C_{H_3} < C_t$. We first take $D = 1$ and $E = 0.4$, which gives that

$$B_1 \approx -2.571408, \quad B_2 \approx -2.641101, \quad B_s \approx -2.320551.$$

Then, $B = -2.6$ is chosen to ensure that the condition (II) is satisfied. Moreover, it is found that

$$X_M \approx 0.635210, \quad X_m \approx 0.704582, \quad X_t = 0.625$$
$$A_H^M \approx 2.055536, \quad A_H^m \approx 2.040534, \quad A_H(X_t) \approx 2.054737.$$

Consequently, $A = 2.0551$ is chosen such that the condition $\max\{A_H^m, A_H(X_t)\} < A < A_H^M$ is satisfied. We choose three particular values for $C$, yielding three different cases. (i) $C = 0.368$ for which the Type-I tristable state exists, as shown in Fig. 6(b) in which

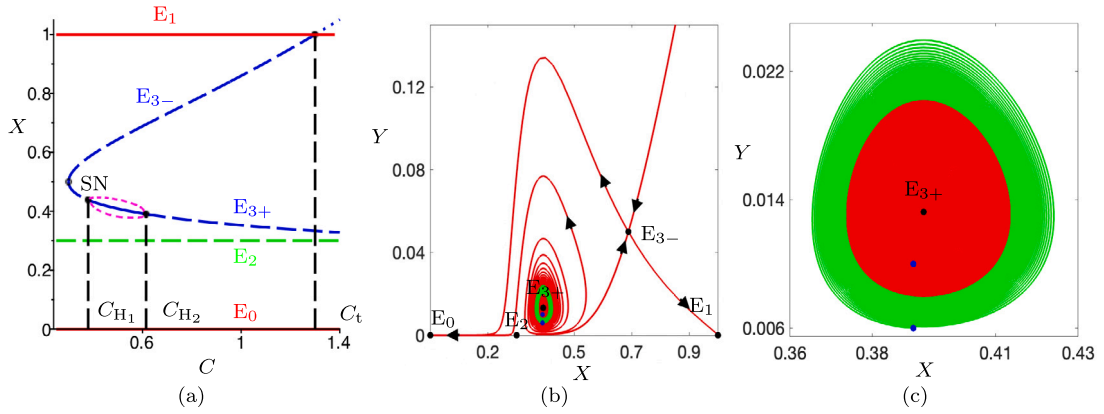


**Fig. 4.** Bifurcation diagram and simulations of system (3) for $A = 4.3$, $B = -4$, $D = 1$, $E = 0.3$: (a) bifurcation diagram projected on the $C$-$X$ plane, where solid and dashed curves represent stable and unstable solutions, respectively; (b) simulated phase portrait for $C = 0.6$ showing one unstable limit cycle; and (c) a zoomed part of the phase portrait in (b), where the unstable limit cycle is approached by the red and green trajectories.

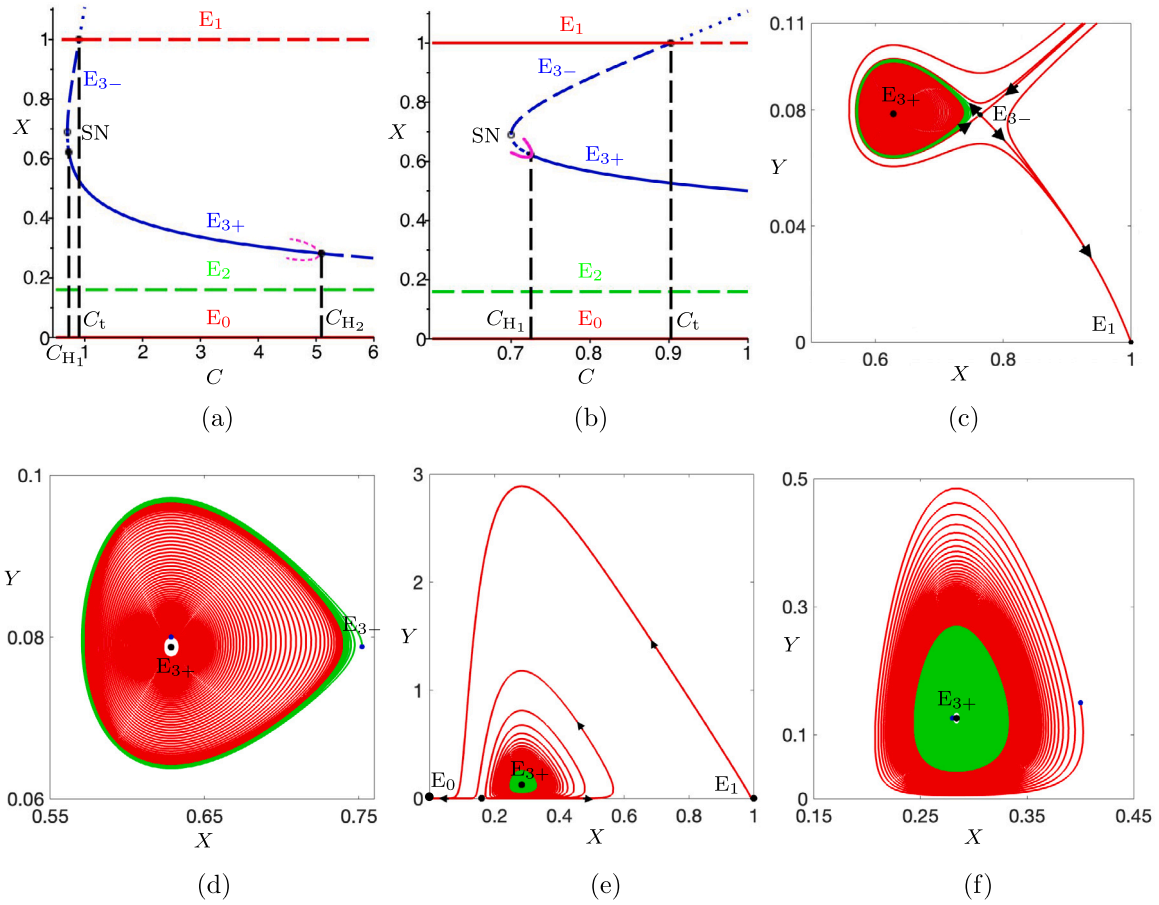


**Fig. 5.** Bifurcation diagrams and simulations of system (3) for $A = 2.8025$, $B = -2.9$, $D = 1$, $E = 0.16$: (a) bifurcation diagram projected on the $C$-$X$ plane, where solid and dashed curves represent stable and unstable solutions, respectively; (b) a zoomed part of the bifurcation diagram in part (a); (c) simulated phase portrait for $C = 0.72$ showing a stable limit cycle; (d) a zoomed part of the phase portrait in part (c); (e) simulated phase portrait for $C = 5$ showing an unstable limit cycle; and (f) a zoomed part of the phase portrait in part (e), where the unstable limit cycle is approached by the green and red trajectories.

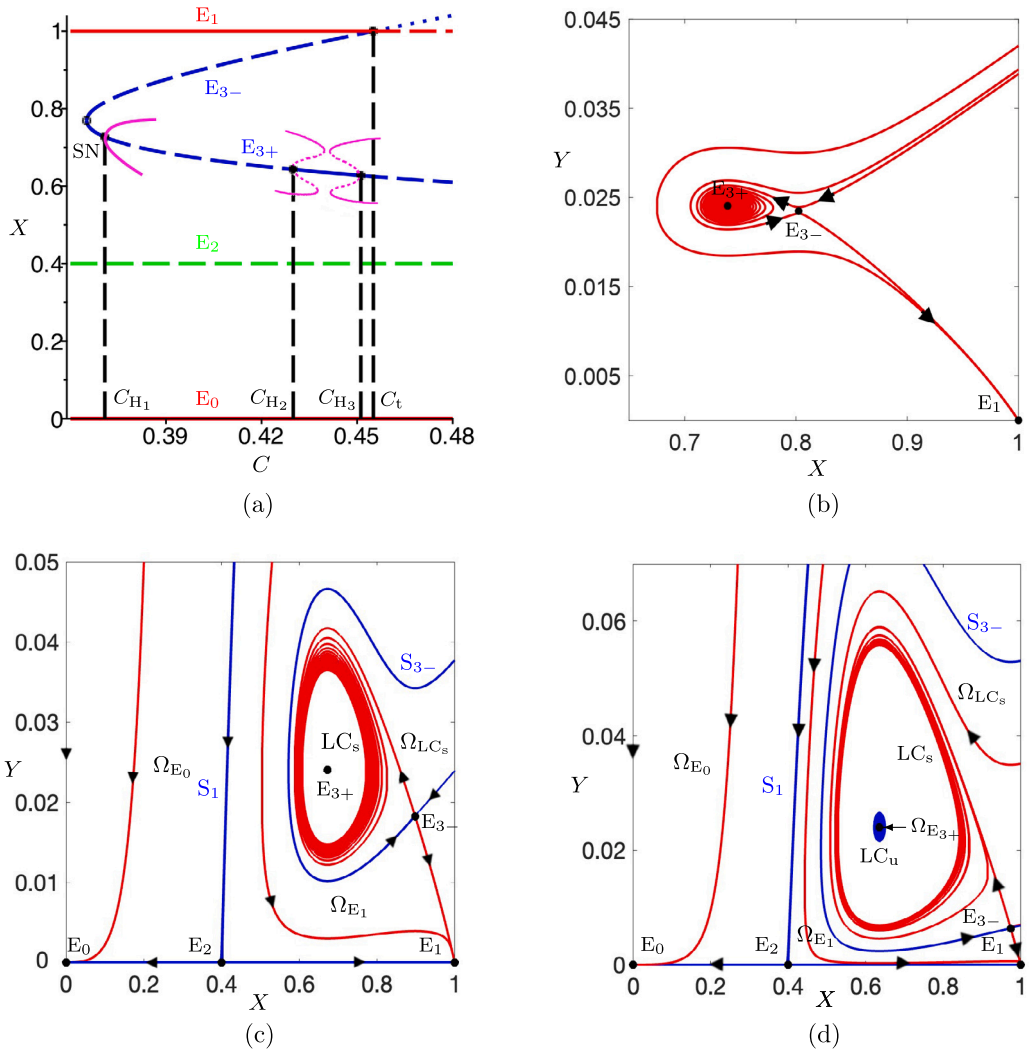


**Fig. 6.** Bifurcation diagram and simulations of system (3) for $A = 2.0551$, $B = -2.6$, $D = 1$, $E = 0.4$: (a) bifurcation diagram projected on the $C$-$X$ plane, where solid and dashed curves represent stable and unstable equilibria, respectively; (b) simulated phase portrait for $C = 0.368$; (c) simulated phase portrait for $C = 0.4$; and (d) simulated phase portrait for $C = 0.44$, where the unstable limit cycle and stable limit cycle are approached by the blue and red curves, respectively.

$E_0$ is not shown. Note that the solution trajectories slowly converge to the focus $E_{3+}$ and converge fast to the node $E_1$. (ii) $C = 0.4$ for which both the Type-I and Type-II tristable phenomena exist, but they are separated in the two sides of the Hopf critical point $C_{H_1}$, see Fig. 6(a). The Type-I tristable states exist on the left side of $C_{H_1}$, consisting of the three AS equilibria $E_0$, $E_1$ and $E_{3+}$. On the right side of $C_{H_1}$, it is seen from Fig. 6(a) that a stable limit cycle $LC_s$ surrounds the unstable focus $E_{3+}$ (see Fig. 6(c)) with coexistence of stable nodes $E_0$ and $E_1$, showing a Type-II tristable state. The simulated phase portrait is shown in Fig. 6(c), where all the trajectories in the region $\Omega_{LC_s}$, bounded by the stable manifold $S_{3-}$ connecting the saddle $E_{3-}$, converge to the stable limit cycle $LC_s$. (iii) $C = 0.44$ for which, again like the case (ii), both Type-I tristable and Type-II tetrastable phenomena occur, but now they can occur on both sides or just one side of the Hopf critical points. Taking a look on the left side of the Hopf critical point $C_{H_3}$ in Fig. 6(a), we can see that a stable focus $E_{3+}$ is surrounded by two limit cycles, as shown in Fig. 6(d), with the inner one $LC_u$ unstable (the blue cycle simulated by using the "backward time" integration scheme) and the outer one $LC_s$ stable (in red color). All the trajectories in the region $\Omega_{E_{3+}}$ converge to $E_{3+}$, while all the trajectories in the region $\Omega_{LC_s}$ bounded by $S_{3-}$ and the unstable limit cycle $LC_u$ converge to the stable limit cycle $LC_s$. Similarly simulated diagrams can be obtained around the Hopf critical point $C_{H_2}$. This illustrates the coexistence of the three AS equilibria, $E_0, E_1$ and $E_{3+}$ (the Type-I tristable phenomenon), as well as the coexistence of the three AS equilibria and the larger stable limit cycle $LC_s$ (the Type-II tristable phenomenon). This can be analytically proved by calculating the first and second focus values at the Hopf bifurcation points, given as follows:

$$\begin{aligned}
&C_{H_1} \approx 0.370805, \quad E_{3H_1} \approx (0.726992, 0.024065), \quad v_1 \approx -0.208041,\\
&C_{H_2} \approx 0.429945, \quad E_{3H_2} \approx (0.643233, 0.0239987), \quad v_1 \approx 0.0491717, \quad v_2 \approx -4.697860,\\
&C_{H_3} \approx 0.451159, \quad E_{3H_3} \approx (0.627605, 0.0239995), \quad v_1 \approx 0.071250, \quad v_2 \approx -4.764436,
\end{aligned}$$

**Table 2**
Multistable states of system (3).

| | | | |
|---|---|---|---|
| Bistable | Type-I | $(E_0, E_1)$, $(E_0, E_{3+})$, $(E_1, E_{3+})$ | Figs. 2, 3(b), 4(b), 5(e) |
| | Type-II | $E_0$ and a stable LC | Figs. 3(c), 5(c), 6(c) |
| Tristable | Type-I | $(E_0, E_1, E_{3+})$ | Figs. 4(b), 5(e) |
| | Type-II | $(E_0, E_1)$ and a stable LC | Figs. 3(c), 6(c) |
| Tetrastable | Type-II | $(E_0, E_1, E_{3+})$ and a stable LC, enclosing an unstable LC and $E_{3+}$ | Fig. 6(d) |

where the focus values at the Hopf critical points $C_{H_2}$ and $C_{H_3}$ satisfy $v_1 \ll -v_2$, which guarantees the existence of two limit cycles.

It should be noted that this Type-II tetrastable phenomenon is different from that shown in part (ii). Here, there exists another unstable limit cycle enclosing the stable equilibrium $E_{3+}$, indicating that the Hopf bifurcation is subcritical. This implies that the codimension of Hopf bifurcation in the system considered in this paper is at least two. Moreover, we conduct numerical simulations to further demonstrate that the codimension-two Hopf bifurcation is only applicable in the cases when the Hopf bifurcation is subcritical. A complete study on the codimension of Hopf bifurcation is out of the scope of this paper.

The above obtained results show that the system (3) can exhibit rich dynamics and multistable states. In a summary, we list all the possible multistable states in Table 2, where LC represents limit cycle.

The multistable phenomenon can cause complex dynamical behaviors and has significant impact on the properties of biological systems. For example, consider the Type-I bistable state, as shown in Fig. 3(b), which, in fact, is also a Type-I tristable case since $E_0$ is also asymptotically stable. Let $S_1$ and $S_{3-}$ denote the stable manifolds connecting the saddles $E_1$ and $E_{3-}$, respectively, see Figs. 3 and 6. Then, $S_1$ and $S_{3-}$ divides the whole $X$-$Y$ plane into three regions, called $\Omega_{E_0}$, $\Omega_{E_1}$ and $\Omega_{E_{3+}}$, which are the trapping areas (or attracting basins) for $E_0$, $E_1$ and $E_{3+}$, respectively, see Fig. 3(b). Therefore, depending upon the initial condition, $I_0 = (X_0, Y_0)$, a trajectory may converge to $E_0$ if $I_0 \in \Omega_{E_0}$, or to $E_1$ if $I_0 \in \Omega_{E_1}$, or to $E_{3+}$ if $I_0 \in \Omega_{E_{3+}}$. This implies the biological implication that due to the coexistence of the three stable equilibria, different initial states which characterize a certain situation of the system, the prey and predator populations may both extinct, or the prey reaches a fixed value but the predator goes to extinction, or both prey and predator coexist and stay in a balanced manner. Such complex dynamical behavior may reflect the real situation in reality. For the type-II tetrastable states, it has one more unstable limit cycle $LC_u$ (see Fig. 6(d)), which is a separatory between the stable equilibrium $E_{3+}$ and the stable limit cycle $LC_s$, leading to one more trapping region $\Omega_{LC_s}$ between $S_{3-}$ and $LC_u$. In this case, more complicated dynamical behaviors including multiple limit cycle bifurcation (oscillation between the populations of prey and predator) show a more complex yet more realistic situation due to the existence of the Allee effect.

## 5. Conclusion and discussion

In this paper, we have investigated a predator–prey system with generalized Holling type III functional response and the strong Allee effect. The hierarchical parametric analysis is applied to obtain explicit conditions in a 5-dimensional parameter space for the existence and stability of equilibrium solutions. In particular, a detailed study on Hopf bifurcation is given to show bifurcation of multiple limit cycles and multistable states. Numerical simulations are conducted to find that the populations of predators and prey can reach a state of periodic fluctuations, which agrees with theoretical predictions from normal forms. The stability analysis shows that the extinction equilibrium is asymptotically stable, implying that both populations tend to go extinct when the population densities are low and subject to a strong Allee effect. Also, the complex dynamics of the predator–prey system are analyzed.

To study the rich dynamics of the system, we first derive the parametric conditions for the existence of biologically meaningful equilibria. It is found that the system has a maximum of five equilibria, two of which are interior equilibria. The hierarchical parametric analysis is used to further study the stability of these equilibria and possible bifurcations. Especially, Hopf bifurcation is proved to appear from the interior equilibrium $E_{3+}$ by choosing the parameter $C$ as the bifurcation parameter. Moreover, explicit expressions given in terms of the parameters are derived to prove that up to three Hopf bifurcation points are possible as $C$ is varied.

An interesting biological behavior has been identified, namely, the system can exhibit multistable states. The method of normal forms is applied to show that codimension-two Hopf bifurcation is possible under certain parameter values. Combining the analytical and numerical studies show that the system admits bistability, tristability and even tetrastability. Simulations show that the system can have two limit cycles, where a large outer stable limit cycle surrounds a small inner unstable limit cycle, and both of them enclose a stable interior equilibrium when the parameters satisfy the codimension-two Hopf condition, and the Hopf bifurcation is subcritical. Note that the origin of the system ($E_0$) is always stable, meaning that populations will both go extinct when the initial populations start close enough to $E_0$ or at any point under the threshold. This also applies to the real situation where a population tends to go extinct when the population size is subject to a strong Allee effect. The dynamical behaviors found in this paper have biological implications:

- Populations reach a stable oscillation ($E_1$ and $E_3$ unstable with a stable limit cycle).
- Both populations ($E_1$ unstable, but $E_3$ stable) coexist.
- Either a stable oscillation of the populations or an extinction of the predator ($E_1$ stable, but $E_3$ unstable, with a stable limit cycle) may occur.
- Either a coexistence of the populations or an extinction of the predator ($E_1$ and $E_3$ stable) happens. A stable oscillation is also possible under certain initial conditions (with codimension-2 Hopf bifurcation).

Compared with the model without the Allee effect [24], the system considered in this paper with the strong Allee effect exhibits more complex dynamical behaviors, including bifurcation of multiple limit cycles and multistable phenomena. Since the system without the Allee effect always has an unstable equilibrium at the origin $(0,0)$, while the system with the Allee effect always has an unstable equilibrium at $(E,0)$, it implies that the dynamical behavior near the origin $(0,0)$ of the former is to appear near the equilibrium $(E,0)$ of the later, causing more complex behaviors due to the additional existence of stable equilibrium $E_0$.

## CRediT authorship contribution statement

**Yanni Zeng:** Formal analysis, Investigation, Software, Validation, Writing – original draft. **Pei Yu:** Conceptualization, Formal analysis, Methodology, Project administration, Supervision, Validation, Writing – review & editing.

## Declaration of competing interest

The authors declare that they have no known competing financial interests or personal relationships that could have appeared to influence the work reported in this paper.

## Data availability

No data was used for the research described in the article.

## Acknowledgments

This work was supported by the Natural Sciences and Engineering Research Council of Canada (No. R2686A02).

## References

[1] Gause GF, Smaragdova NP, Witt AA. Further studies of interaction between predators and prey. J Anim Ecol 1936;5(1):1–18. http://dx.doi.org/10.2307/1087.
[2] Freedman HI. Deterministic mathematical models in population ecology. Pure and applied mathematics, vol. 57, New York: M. Dekker; 1980.
[3] Holling CS. The components of predation as revealed by a study of small-mammal predation of the european pine sawfly. Can Entomol 1959;91(5):293–320. http://dx.doi.org/10.4039/Ent91293-5.
[4] Solomon ME. The natural control of animal populations. J Anim Ecol 1949;18(1):1–35. http://dx.doi.org/10.2307/1578.
[5] Holling CS. Some characteristics of simple types of predation and parasitism. Can Entomol 1959;91(7):385–98. http://dx.doi.org/10.4039/Ent91385-7.
[6] Real LA. The kinetics of functional response. Amer Nat 1977;111(978):289–300. http://dx.doi.org/10.1086/283161.
[7] Lotka AJ. Analytical note on certain rhythmic relations in organic systems. Proc Natl Acad Sci 1920;6(7):410–5. http://dx.doi.org/10.1073/pnas.6.7.410.
[8] Lotka AJ. Fluctuations in the abundance of a species considered mathematically. Nature 1927;119(2983):12. http://dx.doi.org/10.1038/119012a0.
[9] Bazykin AD. Nonlinear dynamics of interacting populations. World Scientific; 1998.
[10] Hassell M, Lawton J, Beddington J. Sigmoid functional responses by invertebrate predators and parasitoids. J Anim Ecol 1977;249–62. http://dx.doi.org/10.2307/3959.
[11] Freedman HI, Wolkowicz GS. Predator-prey systems with group defence: the paradox of enrichment revisited. Bull Math Biol 1986;48(5–6):493–508. http://dx.doi.org/10.1016/S0092-8240(86)90004-2.
[12] Courchamp F, Clutton-Brock T, Grenfell B. Inverse density dependence and the allee effect. Trends Ecol Evol 1999;14(10):405–10. http://dx.doi.org/10.1016/S0169-5347(99)01683-3.
[13] Allee WC. Animal aggregations. Q Rev Biol 1927;2(3):367–98. http://dx.doi.org/10.1086/394281.
[14] Allee WC. Co-operation among animals. Am J Sociol 1931;37(3):386–98. http://dx.doi.org/10.1086/215731.
[15] Stephens PA, Sutherland WJ, Freckleton RP. What is the allee effect? Oikos 1999;185–90. http://dx.doi.org/10.2307/3547011.
[16] Stephens PA, Sutherland WJ. Consequences of the allee effect for behaviour, ecology and conservation. Trends Ecol Evol 1999;14(10):401–5. http://dx.doi.org/10.1016/S0169-5347(99)01684-5.
[17] Lewis MA, Kareiva P. Allee dynamics and the spread of invading organisms. Theor Popul Biol 1993;43(2):141–58. http://dx.doi.org/10.1006/tpbi.1993.1007.
[18] Dennis B. Allee effects: population growth, critical density, and the chance of extinction. Nat Resour Model 1989;3(4):481–538. http://dx.doi.org/10.1111/j.1939-7445.1989.tb00119.x.
[19] Berec L, Angulo E, Courchamp F. Multiple allee effects and population management. Trends Ecol Evol 2007;22(4):185–91. http://dx.doi.org/10.1016/j.tree.2006.12.002.
[20] Zu J, Mimura M. The impact of allee effect on a predator–prey system with holling type ii functional response. Appl Math Comput 2010;217(7):3542–56. http://dx.doi.org/10.1016/j.amc.2010.09.029.
[21] González-Olivares E, Rojas-Palma A. Multiple limit cycles in a gause type predator–prey model with holling type iii functional response and allee effect on prey. Bull Math Biol 2011;73:1378–97. http://dx.doi.org/10.1007/s11538-010-9577-5.
[22] Verma M, Misra A. Modeling the effect of prey refuge on a ratio-dependent predator–prey system with the allee effect. Bull Math Biol 2018;80:626–56. http://dx.doi.org/10.1007/s11538-018-0394-6.
[23] Zeng B, Yu P. A hierarchical parametric analysis on hopf bifurcation of an epidemic model. Discrete Contin Dyn Syst Ser S 2023;16(3 & 4):708–24. http://dx.doi.org/10.3934/dcdss.2022069.
[24] Jiang J, Yu P. Multistable phenomena involving equilibria and periodic motions in predator–prey systems. Int J Bifurcation Chaos 2017;27(03):1750043. http://dx.doi.org/10.1142/S0218127417500432.
[25] Zeng Y, Yu P. Complex dynamics of predator–prey systems with allee effect. Int J Bifurcation Chaos 2022;32(13):2250203. http://dx.doi.org/10.1142/S0218127422502030.
[26] Yu P. Computation of normal forms via a perturbation technique. J Sound Vib 1998;211(1):19–38. http://dx.doi.org/10.1006/jsvi.1997.1347.